ISSN 1069-3513, Izvestiya, Physics of the Solid Earth, 2024, Vol. 60, No. 1, pp. 8–31. © Pleiades Publishing, Ltd., 2024.
Russian Text © The Author(s), 2024, published in Fizika Zemli, 2024, No. 1, pp. 11–36.

# Anomalous Features in the Behavior of the Geomagnetic Field at the End of the Cretaceous Normal Superchron: Insights from the Study of the Turonian–Santonian in the Southwestern Crimea

**A. Yu. Guzhikov[a], *, E. Yu. Baraboshkin[b, c], **, I. P. Ryabov[a], ***, M. A. Ustinova[c], ****, and V. S. Vishnevskaya[c], *****

[a] *Saratov State University, Saratov, 410012 Russia*
[b] *Faculty of Geology, Moscow State University, Moscow, 119991 Russia*
[c] *Geological Institute, Russian Academy of Sciences, Moscow, 119017 Russia*
**e-mail: aguzhikov@yandex.ru*
***e-mail: ejbaraboshkin@mail.ru*
****e-mail: ryaboff.il@yandex.ru*
*****e-mail: ustinova_masha@mail.ru*
******e-mail: valentina.vishnaa@mail.ru*

Received April 7, 2023; revised June 5, 2023; accepted June 8, 2023

**Abstract**—In 394 samples characterizing 266 stratigraphic levels in four Turonian–Santonian sections of the Southwestern Crimea, characteristic remanent magnetization components (ChRM) acquired at the stage of diagenesis are identified. The obtained data fix the record of the paleosecular geomagnetic variation of high amplitude (root mean square deviation $S = 25.9°$ with a fixed cut-off angle of 45°, which is about twice as high as the model $S$ for this latitude) in the sediments formed during ~5–6 Myr and is interpreted as anomalous behavior of the geomagnetic field in the Turonian, Coniacian, and Santonian.

**Keywords:** paleomagnetism, fine structure of the field, Cretaceous normal polarity superchron, magnetostratigraphy, Upper Cretaceous, Turonian, Coniacian, Santonian, benthic foraminifera, calcareous nannoplankton, gilianelles, ammonites

**DOI:** 10.1134/S1069351324700150

## INTRODUCTION

Previous studies revealed an anomalously large scatter of paleomagnetic directions in the Upper Turonian–Santonian sediments of the Aksu-Dere ravine section, southwestern Crimea (Guzhikov and Feduleev, 2019; Guzhikov et al., 2021b). The observed feature has not been definitely explained due to the lack of data to reliably substantiate the primary nature of the characteristic magnetization components (ChRM). In particular, it was not possible to determine the age of ChRM due to inapplicability of standard field tests. The reversal test could not been applied because the Turonian–Santonian in the SW Crimea is covered by a magnetozone of normal polarity. Furthermore, the overlying Campanian–Maastrichtian sediments where magnetozones of reversed polarity were encountered are partially remagnetized, making it impossible to identify ancient magnetization components in a “pure” form (Baraboshkin et al., 2020; Guzhikov et al., 2021b; Guzhikova, 2018). The fold test proved not to work due to small variations in bedding attitudes of layers. Although there are indirect data suggesting primary origin of the magnetization, they are insufficient to draw unambiguous conclusions about the nature of the ChRM. Therefore, along with the hypothesis that significant variations in paleomagnetic vectors were caused by the anomalous behavior of the geomagnetic field, other ideas related to partial remagnetization of rocks were not excluded.

The demonstrable evidence that the field behaved unusually during a period of 5–6 Myr from the end of the Turonian to the end of the Santonian (Gradstein et al., 2020) could be provided by tracing similar high-amplitude ChRM variations in the coeval sediments of other sections. The dedicated studies of the Turonian in the Kizil-Chigir section (~8.5 km north of the Aksu-Dere section) and the Santonian in the Kudrino-2 section (~2.2 km south of the Aksu-Dere section) revealed high values of the concentration parameters (Guzhikov and Feduleev, 2019; Guzhikov et al., 2021b; 2020). However, subsequently it was established that, compared to Aksu-Dere, the Turonian layers present in the Kizil-Chigir section are older (the age is determined by I.P. Ryabov based on the benthic foraminifera (BF) data presented in this paper), while the Santonian rocks present in the Kudrino-2 section are younger than in Aksu-Dere (Guzhikov et al., 2021a; 2021b). Thus, the question of whether the paleomagnetic variations are laterally stable remained open. A significant scatter of ChRM was detected in a thin (~2 m) Aksu-Dere-2 outcrop of the Coniacian and Santonian boundary layers, located close (~1.4 km) to the Aksu-Dere section (Guzhikov and Feduleev, 2019). However, since only six levels were sampled in this outcrop and it is located close to the main section do not allow the data for Aksu-Dere-2 to be considered a strong argument in favor of the anomalous behavior of the Late Cretaceous field.

For identifying the nature of high-amplitude variations in paleomagnetic directions, the data for the Santonian of the Chuku Mountain section in the Belbek–Kacha interfluve are crucial. These data document the record of the variations in paleomagnetic directions similar to those previously identified in Aksu-Dere (Guzhikov and Feduleev, 2019; Guzhikov et al., 2021b). At the same time, the top layers of the Chuku section, which are the age analog of the top Santonian sediments in the Kudrino-2 section, are characterized by high concentration of the directions.

Detailed results of the integrated biostratigraphic and magnetostratigraphic studies for the Santonian of the Aksu-Dere–Kudrino composite section are described in the previous papers (Guzhikov et al., 2021a; 2021b), and a brief summary of the paleomagnetic and micropaleontological data was published for the Turonian–Coniacian part of the Aksu-Dere section (Guzhikov and Feduleev, 2019; Guzhikova et al., 2020), Kizil-Chigir and Chuku sections (Guzhikova et al., 2021).

This work presents the detailed paleomagnetic and rock magnetic data for the Turonian–Coniacian of the Aksu-Dere section and for the Turonian of the Kizil-Chigir section (A.Yu. Guzhikov), which are published for the first time. The brief micropaleontological characterization of the Turonian–Santonian of the Kizil-Chigir and Chuku sections (I.P. Ryabov, M.A. Ustinova, V.S. Vishnevskaya), the redeterminations of ammonites from V.G. Klikushin's collection and sedimentological characterization of the sections (E.Yu. Baraboshkin) are also presented for the first time.

## GEOLOGICAL CHARACTERIZATION OF THE STUDIED SECTIONS

The Turonian, Coniacian, and Santonian stages in the southwestern part of the Mountain Crimea are mainly represented by limestones and are quite similar by lithology. The lower Turonian, rich in terrigenous material, is part of the Belogorskaya Formation; the middle–upper Turonian and Coniacian constitute the Prokhladnenskaya Formation, and the Santonian, composed of less hard limestones compared to the Turonian–Coniacian limestones, belongs to the Kudrinskaya Formation (Plotnikova et al., 1984; Alekseev, 1989). The Turonian–Santonian units, as well as the entire Upper Cretaceous, are part of the subplatform complex (Cretaceous–Eocene), which overlies the Cimmerian folded basement in a monocline manner. The strata generally dip to the northwest, with local variations in dip direction from west to north; the dip is predominantly gentle (10° to 15°). Only at the southern edge of the monocline do dip angles increase sharply, up to subvertical bedding (Table 1). Compared to the Santonian and Coniacian, which are partially or completely destroyed by the scouring action of the Santonian and Pre-Campanian erosion, the Turonian is most abundant in the southwestern Crimea (Alekseev, 1989).

We have studied four Turonian–Santonian sections in the Bakhchysarai region. The Kizil-Chigir section (outcrops 3186, 3172) is located on the western slope of the mountain of the same name on the northern outskirts of the village of Trudolyubovka on the right bank of the Bodrak river. The Kudrino-2 section (outcrop 3184) on the northern outskirts of the Kudrino village and the Aksu-Dere ravine section (outrcop 3168) approximately 2 km north of the village are located on the right side of the Kacha River valley. The Chuku section near the Vysokoe village was sampled on the southern and eastern slopes of Mount Chuku (also known as Polyus), which is part of the Kacha–Belbek river watershed (Fig. 1, Fig. 2, Table 1).

One of the regions with the most comprehensive paleontological characterization is the Aksu-Dere ravine section, where we sampled the interval from the Upper Turonian to the Santonian, with an apparent thickness of 16.5 m (Fig. 2e, Fig. 3). The Late Turonian–Early Coniacian age of the rocks is substantiated by the inoceramid–planktonic foraminiferal biostratigraphy studies (Kopaevich and Walaszczyk, 1990; 1993). More recent studies in this section have established the presence of middle Coniacian and a possible presence of upper Coniacian strata (Guzhikova et al., 2020; Scherbinina and Gavrilov, 2018). The base of the Santonian (the boundary of the Prokhladnenskaya and Kudrinskaya formations) is defined by the mature surface and is readily identified in the adjacent (~1.4 km to the south) thin (apparent thickness 2.1 m) Aksu-Dere-2 outcrop, where paleomagnetic sampling of the upper Coniacian layers and lower Santonian layers was duplicated. The Lower Santonian is missing in the section; the late Santonian age of the rocks and the location of the Santonian–Campanian boundary in the section are established based on the combination of bio-, chemo- (stable isotopes of

**Table 1.** Section information

| Section name (Outcrop no.) | Geographic corordinates | | Age | Thickness, m/Number of levels | Measured/**averaged***** azimuth(s) and dip angle(s), deg |
|---|---|---|---|---|---|
| | Latitude, N | Longitude, E | | | |
| Chuku **(3180)** | 44°38′11.2″ | 33°56′20.5″ | Late Santonian | 0.7/12 | 162–318 ∠5–80 |
| Chuku (3175) | *44°38′11.0″<br>**44°38′10.5″ | 33°56′22.3″<br>33°56′13.1″ | | 44.6/45 | 187–347 ∠3–28/**300 ∠19** |
| Chuku (3181) | *44°38′11.8″<br>**44°38′09.9″ | 33°56′31.3″<br>33°56′30.6″ | | 29.2/32 | 185–240 ∠15–55/**208 ∠33** |
| Chuku (3177, samples 1–47) | *44°37′48.2″<br>**44°37′52.1″ | 33°56′24.4″<br>33°56′20.3″ | | 96.4/31 | 282–334 ∠20–50/**309 ∠35.5** |
| Chuku (3177, samples 48–78) | *44°37′37.5″<br>**44°37′38.1″ | 33°56′22.5″<br>33°56′19.3″ | Early(?)–Late Santonian | 40.7/47 | 287–342 ∠38–85/**320 ∠69** |
| Chuku (3176) | *44°38′07.6″<br>**44°38′06.3″ | 33°56′28.5″<br>33°56′27.9″ | Turonian (?) + Campanian (?) | 13.0/18 | 277–317 ∠10–14/**292 ∠13** |
| Kudrino-2 (3184) | *44°42′15.0″<br>**44°42′17.8″ | 33°56′49.5″<br>33°56′47.6″ | Late Santonian | 23.7/27 | 292–346 ∠10–19/**312 ∠14** |
| Aksu-Dere (3168) | *44°43′27.0″<br>**44°43′26.9″ | 33°56′52.0″<br>33°56′54.6″ | Late Turonian–Coniacian + Late Santonian | 16.7/69 | 317–17 ∠6–21/**344 ∠11** |
| Kizil-Chigir (3186, 3172) | *44°47′43.0″<br>**44°47′42.2″ | 33°59′18.5″<br>33°59′20.7″ | Early–Middle(–Late?) Turonian | 11.1/23 | 342–2 ∠14–15/**357 ∠14** |

* Start of sampling; ** End of sampling; *** averaged attitudes adequately reflect the dominant dips of the beds, which are clearly expressed in all outcrops except for 3180 (subaqueous slump fold).

carbon, oxygen, and strontium), and magnetostratigraphic data (Guzhikov et al., 2021a; 2021b).

The Santonian–Campanian boundary interval contains clear signs of hiatuses (including erosion) in sedimentation and condensation in the Aksu-Dere section, but is more fully preserved in the Kudrino-2 section (Fig. 3) located ~2.2 km to the south. Based on the integrated studies, it was established that in the Kudrino-2 section, the most magnetostratigraphically fully explored are the younger Santonian strata whose analogs are missing in the Aksu-Dere section (Guzhikov et al., 2021a; 2021b).

The Kizil-Chigir section (Fig. 3) includes the Turonian Prokhladnenskaya Formation with an apparent thickness of 17 m, which is overlain by the Campanian Kudrinskaya Formation with no signs of angular unconformity but with a hiatus. The top layers of the Prokhladnenskaya Formation were traditionally attributed to the Upper Turonian (Alekseev, 1989; Baraboshkin et al., 2016), but our studies have shown the presence of the BF assemblage there, characteristic of the lower Turonian Substage. In the lower part of the section (sample 3186-1), *Gyroidina nitida* (Reuss), *Tappanina eouvigeriniformis* (Keller), *Cibicides pollyrraphes* (Reuss), *Gyroidina lenticula* (Reuss) and other species characteristic of the lower Turonian of the East European Platform, Crimea, and Mangyshlak were found. Higher in the section, in sample 3186-6, numerous occurrences of *Stensioeina* (*Protostensioeina*) *granulata humilis* (Koch), as well as *Marssonella oxycona* (Reuss), *Berthelina berthelini* (Keller), etc., are noted. Further up in the section (sample 3186-17), *Reussella carinata* (Vasilenko) appears, which is a descendant of *R. turonica*.

Thus, in the Kizil-Chigir section, three BF complexes can be distinguished in the rank of layers, which correlate with the zonal scheme of the East European Platform (Benyamovsky, 2008): layers with *Tappanina eouvigeriniformis* (Gavelinella nana LC3 zone, lower Turonian), beds with *Stensioeina* (*Protostensioeina*) *granulata humilis*/*Reussella turonica* and beds with *Reussella carinata* (Protostensioeina praeexculpta LC5 zone, middle–upper Turonian) (Fig. 3).

The presence of the lower Turonian BF forms in the complex, which have not been detected in the Aksu-Dere section (Guzhikova et al., 2020), suggests that the upper layers of the Prokhladnenskaya Formation in the Trudolyubovka region are more ancient and belong to the lower–middle Turonian.

From the literature data (Klikushin, 1985; Alekseev, 1989) it is known that the most complete Turonian–Santonian sections are located on the watershed of the Kacha and Belbek rivers, including those on the Chuku Mountain. V.G. Klikushin who thoroughly studied the Turonian–Santonian sediments of the Belbek River basin did not detect on Mount Chuku any indications of a significant hiatus associated with the Santonian erosion, which is widespread in the southwestern Crimea.

Based on the macrofaunistic data (crinoids, inoceramids, echinoids, ammonites, and brachiopods), Klikushin (1985) identified 11 m thick Turonian, 20 m thick Coniacian, and 37 m thick Santonian strata in

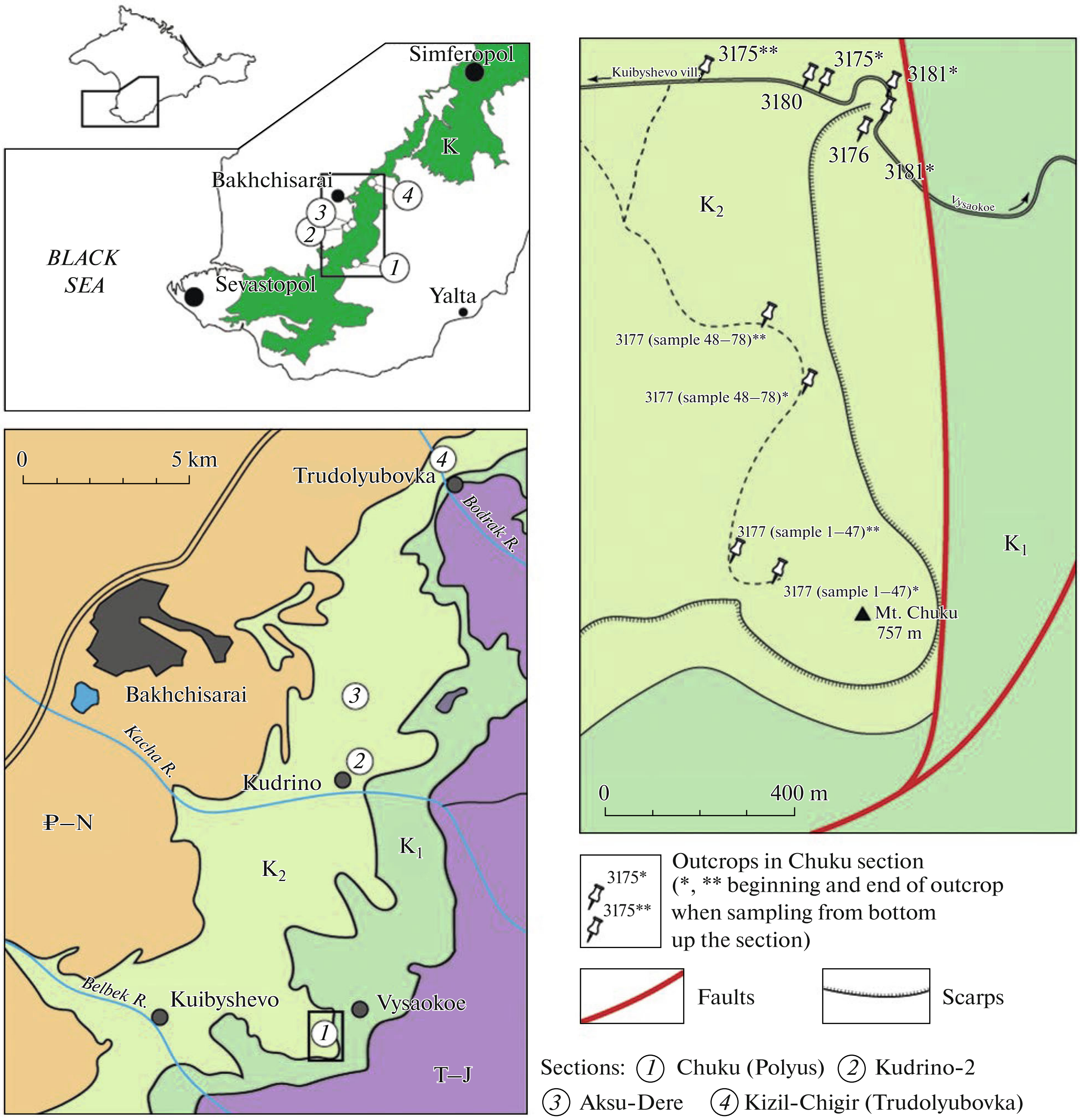


**Fig. 1.** Schematic geological map of study region, with locations of surveyed sections and outcrops. Schematic geological map of Mt. Chuku region is after (Yudin, 2020).

the Chuku section. Later, Bragina and Bragin (2007) studied radiolarian assemblages from the same sections, which confirmed only the middle Turonian and lower Coniacian age of the sediments.

We had a small collection of ammonites the determinations of which, made by A.A. Atabekyan (VSEGEI) and A.S. Alekseev (MSU), are presented in (Klikushin, 1985). Although the exact position of ammonites in the sections is unknown, we were able to determine their age. The late Turonian age was confirmed by the finds of *Puzosia* (*Puzosia*) cf. *muelleri* De Grossouvre and *Tongoboryceras* sp. juv., and the late Santonian age was confirmed by the ammonite assemblage *Hauericeras (Gardeniceras) gardeni* (Baily), *"Nowakites" katschthaleri* (Immel, Klinger et Wiedmann), *Baculites incurvatus* Dujardin, *Pseudoxybeloceras (Parasolenoceras) splendens* Collignon and others. The presence of Coniacian and lower Santonian sediments has not yet been confirmed by ammonites.

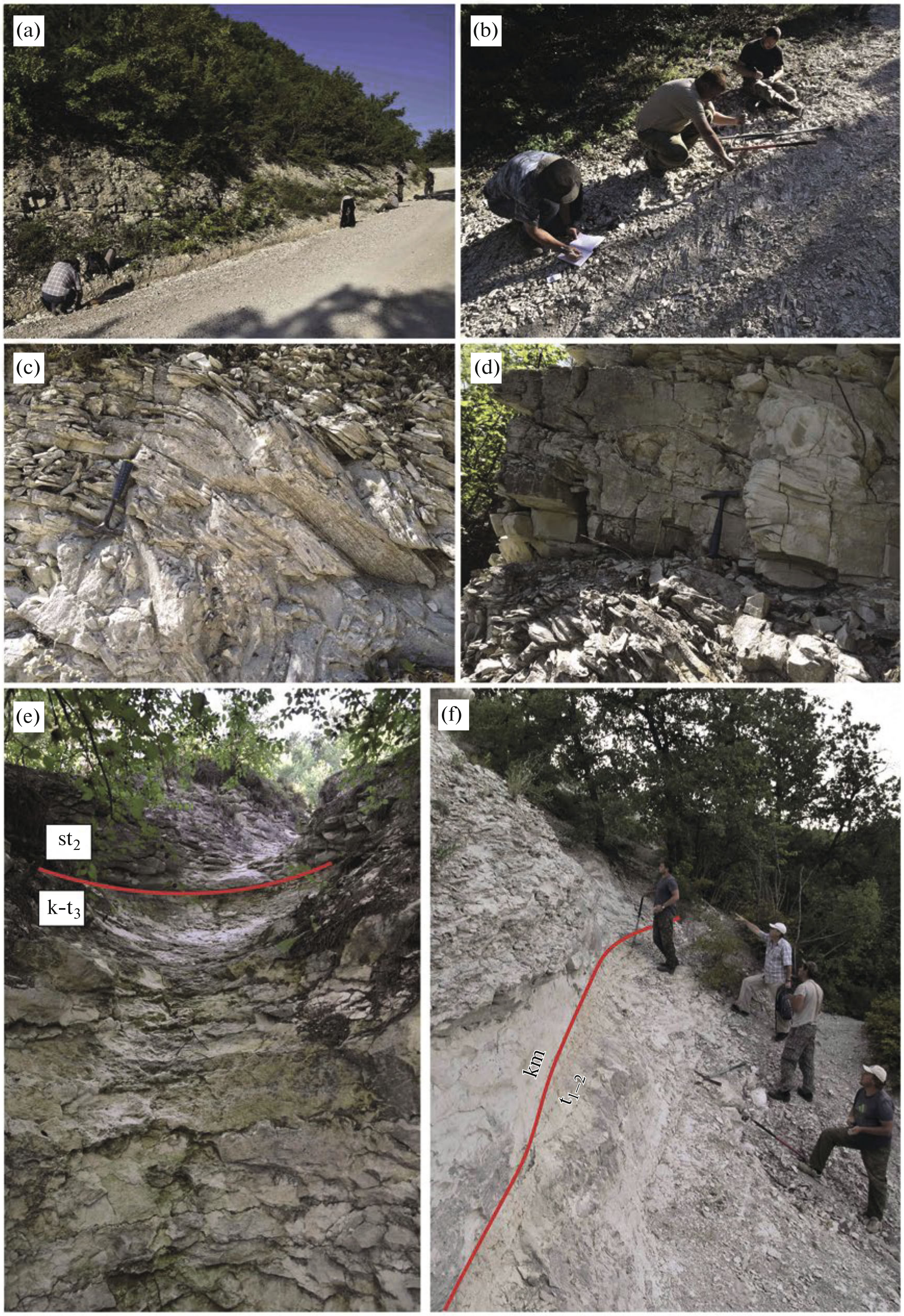


**Fig. 2.** Photographs of surveyed outcrops in Chuku section: (a) outcrop 3175 (upper Santonian); (b) outcrop 3177 (samples 1–47) (lower(?)–upper Santonian); (c) outcrop 3180 (upper Santonian); (d) outcrop 3176 (Santonian?); (e) Aksu-Dere section (outcrop 3168, upper Turonian–Coniacian and base of upper Turonian); (f) Kizil-Chigir section (outcrop 3172, boundary between Turonian and Campanian).

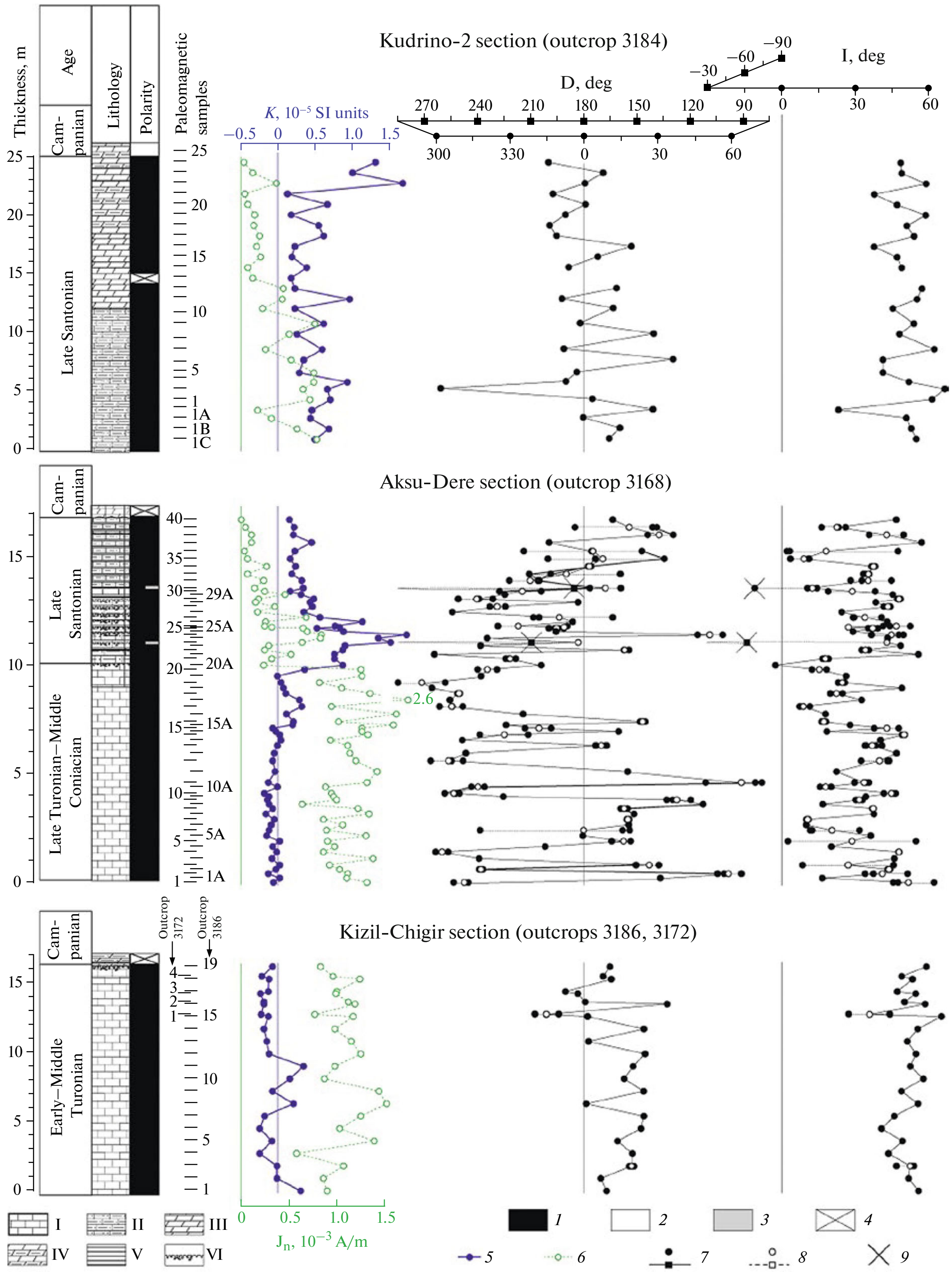


**Fig. 3.** Magnetostratigraphic characteristics of Turonian–Santonian of Kizil-Chigir, Aksu-Dere, and Kudrino-2 sections. Lithology: I, limestones; II, silty limestones; III, marls; IV, strongly clayey marls; V, clays; VI, hardgrounds. Polarity: *1*, normal; *2*, reversed; *3*, anomalous; *4*, no polarity data. Graphs for sections: *5*, magnetic susceptibility *K*; *6*, natural remanent magnetization $\mathbf{J_n}$; *7*, paleomagnetic declination D and inclination I; *8*, average paleomagnetic vectors from samples from same level (circles and squares correspond to ranges 285° < D < 360°, 0° ≤ D < 75°, (–30°) < I < 90° and 75° ≤ D ≤ 285°, (–90°) < I < (–30°), respectively); *9*, paleomagnetic directions excluded from statistical analysis.

The lower and upper parts of the section described in (Klikushin, 1985) were sampled in outcrops 3176 on the steep eastern slope of Chuku Mountain and 3175 on the southern slope, along the road Vysokoe–Kuibyshevo villages (Figs. 2a, 2d). In this section, benthic foraminifers *Gavelinella ammonoides* and *Marssonella oxycona* were encountered only in sample 3176-3, suggesting the early to middle Turonian age of the section base. Up the section, M.A. Ustinova identified a nannoplankton assemblage with *Zeugrhabdotus scutula* and *Eprolithus moratus*, based on which the middle part of the section (samples 3176-4-3176-14) was attributed to the Santonian. Further up in the sequence, above the well pronounced erosion surface, *Arkhangelskiella* sp. occur in the depleted nannoplankton assemblage, presumably testifying to the early Campanian age of the rocks (samples 3176-15 to 3176-18).

Judging by its thickness (44.6 m), outcrop 3175 should represent both Santonian substages, because, according to Klikushin (1985), the lower Santonian strata are 16 m thick, and the apparent thickness of the upper Santonian strata is 21 m. However, the BF assemblage recognized from this outcrop is typical only for the upper Santonian. The assemblage includes, inter alia, *Heterostomella praefoveolata*, previously known in Crimea only from the beds of the same name of the Kudrino-2 section, corresponding to the uppermost Santonian (Guzhikov et al., 2021a; 2021b). In outcrop 3175, planktonic foraminifera (PF) *Sigalia carpathica* (Salaj et Samuel), *S. decoratissima* (de Klasz) were identified, which are characteristic of the upper part of the Dicarinella asymetrica zone (Coccioni et al., 2015), which spans the uppermost portion of the Santonian. This may indicate the presence of even younger sediments here than in Kudrino-2, where the above PFs were not detected (Guzhikov et al., 2021a; 2021b). The Santonian age is not in question by our finding of the *Eupachydiscus* sp. ammonite from the lower part of the section (sample 3175-3).

In search of Coniacian–lower Santonian deposits, we have surveyed a section in a dirt road leading through the forest along the western slope of Chuku Mountain to its top (outcrop 3177) (Fig. 2b). According to (Yudin, 2020), the Cretaceous sediments are here deformed into a thrust fold, and, with a general west-northwestern dip direction of layers being maintained, the dip angles gradually become shallower from the mountain's top to the foot. At the top of the mountain (in the interval between samples 3177-1 and 3177-47), the average dip angle is almost 70°, in the middle of the slope (interval between samples 3177-48 and 3177-78) it is ~40°, and at the foot (outcrop 3175) it is 13°–17° (Table 1, Figs. 1, 2a, 2b, 2d). The significant variations in the dip azimuths and dip angles relative to the mean bedding attitude (Table 1) are probably related to the widespread occurrence of syngenetic landslide deformations in the section (Figs. 2c, 2d).

Based on the BFs, the upper part of outcrop 3177, starting from the level of sample 3177-40, should be attributed to Upper Santonian as suggested by the occurrence of *Heterostomella praefoveolata* and the presence of planktonic foraminifera *Sigalia decoratissima* (sample 3177-57). The BF assemblage in the lower part of outcrop 3177 is represented by *Gavelinella stelligera*, *Stensioeina gracilis*, *S. perfecta*, etc., which suggests the Santonian age of the sediments and raises doubts about the presence of the Coniacian.

Furthermore, in samples 3177/32, 3177/36, 3177/43, 3177/45, V.S. Vishnevskaya identified calcareous microproblematics: gilianella (*Azymella cannabinata* Odin, *Gilianella tenuibrachialis* Odin, *Numismella tarbellica* Odin and others). These species are widespread mostly in the Campanian, which supports the generally Late Santonian–Campanian age of the studied section.

Thus, we did not confirm the presence of the Coniacian and lower Santonian units on Mt. Chuku, perhaps due to the outcrop degradation over the last 40 years. The results of the field studies revealed a new problem: the thickness of the Santonian sediments sampled in outcrop 3177 is ~90 m, and, considering the hiatuses in the exposure, at least 140 m. Even if we assume that outcrop 3177 does not build up the section but replicates outcrop 3177, the thickness measured by our survey is still many times greater than the thickness of the Santonian strata indicated by the author of the first description of the section. Given the fragmentary exposure and complex geological structure of the study region, we can assume that the sampling procedure may have captured the same intervals of the section twice due to the presence of faults or syngenetic deformations (subaqueous slump folds) which are widespread in the studied sediments (Figs. 2c, 2d). These same factors may have resulted in the reduction of substantial intervals of the section described in (Klikushin, 1985), but additional studies are required to elucidating the causes of the inconsistencies.

The Santonian rocks on Chuku Mountain are rather homogeneous, with no reliable lithologic or petromagnetic markers (Fig. 4). However, according to the results of the paleomagnetic studies described below in the section "Results," the possibility of duplication of layers is excluded, at least for outcrops 3177 and 3175. It seems more likely that fragments of the section were reduced due to faults or/and the presence of significant changes in the thickness of the coeval layers.

On Mt. Chuku, we also tested outcrop 3181 on the eastern side of the characteristic loop-shaped bend in the Kuibyshevo–Vysokoye road (Fig. 1). Here, along the road, the rocks are exposed that are indistinguishable in appearance from the Santonian limestones studied in outcrops 3175 and 3177. The assemblage of benthic foraminifers encountered in outcrop 3181 is identical to the BF assemblage revealed in outcrop 3175. The paleomagnetic and rock magnetic data (see

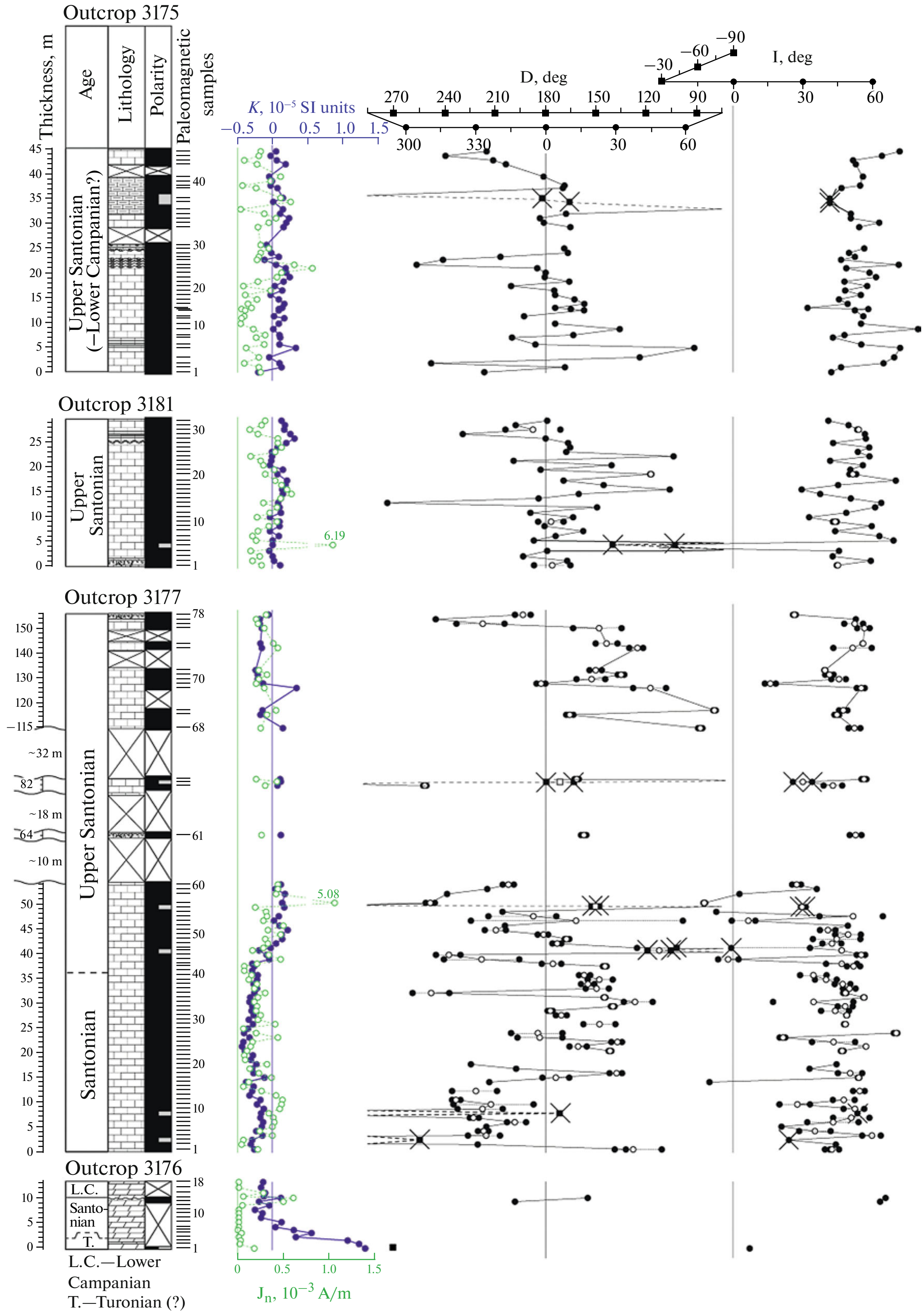


**Fig. 4.** Magnetostratigraphic characteristics of Turonian(?) and Santonian sections in Mt. Chuku region. Designations are same as in Fig. 3. Wavy lines in outcrop 3177 are boundaries of exposure hiatuses, thicknesses shown out of scale. Relative locations of outcrops 3176, 3175, 3181, and 3177 are shown in Fig. 10.

the “Results“ section) are consistent with the idea that layers in outcrops 3175 and 3181 are coeval.

Within outcrop 3175, as a separate object of paleomagnetic studies (outcrop 3180), a subaqueous slump fold was identified (Fig. 2c). Oriented samples were taken from the fold limbs and examined to determine the mechanism of magnetization acquisition during deformation of incompletely lithified layers of carbonate sediments. We note that similar folds were detected in section 3176 at the Santonian base (Fig. 2d), in the lower Turonian Aksu-Dere sediments and in other Turonian–Santonian sections.

## FIELD PROCEDURE AND LABORATORY MEASUREMENTS

In each section studied, in parallel with its detailed (layer-by-layer) description and search for macrofaunal remains, samples were collected taken for various types of analyses on a sample-to-sample basis. For paleomagnetic studies, hand samples were collected using entrenching tools, from which three to four 2 × 2 × 2 cm cubic specimens were subsequently cut, or oriented cores with a diameter of 2.5 cm were drilled with Drill Core D261-C, from which 2.2 cm high cylinders were made. Depending on the thickness of stratigraphic units, paleomagnetic sampling interval ranged from 0.2–0.3 to 0.9–1.2 m (Table 1). Each level was sampled for petrographic studies and isotopic geochemical analyses, and each fifth level was sampled for micropaleontological analyses (planktonic and benthic foraminifers, dinocysts, and nannoplankton).

In the Upper Turonian–Santonian interval of the Aksu-Dere section, in which the 2018 paleomagnetic study revealed ChRM variations of anomalously high amplitude (Guzhikov and Feduleev, 2019), oriented samples were additionally collected from another 29 levels in 2019 to validate the detected effect. Measurements of bedding attitudes during the repeat sampling of the section have been carried out with special care to avoid the false effect of significant scatter in ChRM resulting from misinterpreting surfaces of other nature (e..g., those produced by tectonic fracturing) as bedding planes.

The rock magnetic and magnetic mineralogy studies involved measuring natural remanent magnetization ($\mathbf{J_n}$), bulk magnetic susceptibility ($K$) of rocks before and after heating at 500°C for an hour, anisotropy of magnetic susceptibility (AMS), magnetic hysteresis parameters, and coercivity.

Most of the research was carried out in the Laboratory of Petrophysics of Saratov State University. Magnetic susceptibility was measured on a kappabridge MFK1-FB (AGICO, Czech Republic) with a sensitivity of $3 \times 10^{-8}$ SI units for $K$ and $2 \times 10^{-8}$ SI units for AMS. Remanent magnetization measurements were carried out with a spin magnetometer JR-6 (AGICO, Czech Republic) with a sensitivity of $2 \times 10^{-6}$ A/m. Hysteresis characteristics were determined using a controlled electromagnet with a maximum field intensity of 700 mT. Heating of samples to 500°C was carried out in SNOL-6/11-V muffle furnaces.

In selected samples, the temperature ($T$) dependences of $K$ were studied in the Laboratory of Geodynamics and Paleomagnetism of the Trofimuk Institute of Petroleum Geology and Geophysics of the Siberian Branch of the Russian Academy of Sciences (INGG SB RAS) on the MFK1-FA kappabridge with CS3 temperature control unit (AGICO, Czech Republic). Selected samples were also tested on the coercivity spectrometer J_meter in the Laboratory of Paleoecology, Paleoclimatology and Paleomagnetism of the Kazan Federal University and on the TESCAN-VEGA II microanalyzer in the Geophysical Laboratory “Borok” of Schmidt Institute of Physics of the Earth of the Russian Academy of Sciences (IPE RAS).

Paleomagnetic studies followed the standard procedure (Khramov et al., 1982) involving $\mathbf{J_n}$ measurements in oriented samples on a spin magnetometer JR-6 after their successive demagnetization by an alternating field (AF) on the LDA-3 AF demagnetizer and by thermal demagnetization in a furnace designed by Aparin. Paleomagnetic studies of selected samples were duplicated on a cryogenic magnetometer SQUID 2G-Enterprices at IPE RAS. The data obtained using different demagnetization methods and on different instruments have shown good consistency.

Paleomagnetic laboratory processing was conducted for one to four samples per level from the Upper Turonian–Santonian Aksu-Dere section and for one or two samples per level from outcrop 3177 of the Chuku section. In the other sections/outcrops, AF or thermal demagnetization processing was carried out for one sample from each level.

Remanence components were analyzed using Remasoft 3.0, the paleomagnetic software package developed by Chadima and Hrouda (2006). The analysis of AMS data was performed using Anisoft 5.1.03 software from agico.com.

The techniques employed for the laboratory bio- and magnetostratigraphic studies of the Kizil-Chigir and Chuku sections and Upper Turonian–Coniacian part of the Aksu-Dere section were identical to those used for studying the Santonian of the Aksu-Dere and Kudrino-2 sections described in detail in (Guzhikov et al., 2021a; 2021b).

The fold test was conducted by the algorithm proposed by McFadden (1990).

The fine structure of the field was quantitatively analyzed both over the entire set of directions and based on the samples where virtual geomagnetic poles (VGPs) deviating from the mean VGP by more than 45° were preliminarily excluded. Such a cut-off is necessary to estimate the amplitude of paleosecular variation during “normal” epochs (neither excursions, nor reversals) (Lebedev et al., 2022; McElhinny and McFadden, 1997).

As a measure of the amplitude of paleomagnetic variations, we used the root mean square deviation:

$$S = \left[\frac{1}{N-1}\sum_{i=1}^{N}\left(\Delta_i^2\right)\right]^{1/2} \quad (i = 1,\ldots,N), \qquad (1)$$

where $N$ is the number of stratigraphic levels at which ChRMs are identified; $\Delta_i$ is the angular distance from the $i$th VGP, calculated for each $i$th level from the mean ChRM at that level, to the mean VGP (Cox, 1990).

## RESULTS

The surveyed sections, with the exception of outcrop 3176 at Mt. Chuku, are similar in magnetic properties and are generally favorable for paleomagnetic studies. The characteristic magnetization components were isolated in approximately 95% of the total volume of the examined collection.

The results of the rock magnetic, magnetic mineralogy, and paleomagnetic studies of the Santonian, represented only by its upper substage, in the Aksu-Dere and Kudrino-2 sections were described in detail in the previous paper (Guzhikov et al., 2021b). The main carrier of magnetization in these sediments is finely dispersed pseudo single domain (PSD) magnetite, presumably biogenic. Magnetic susceptibility ($K$) varies from 0.1 to 1.7 × $10^{-5}$ SI units, natural remanent magnetization ($\mathbf{J_n}$) ranges from 0.1 to 0.8 × $10^{-3}$ A/m (Fig. 3). The rocks show a clear paleomagnetic signal; ChRMs with maximum angular deviation (MAD) from 0.5° to 4° are reliably isolated in them. The magnetization is single component or dual component, the latter is more characteristic of the upper part of the Santonian.

The magnetic properties of the Turonian–Coniacian strata of the Aksu-Dere section and the Santonian rocks of the Chuku section, which are presented in this paper for the first time, are very similar to the paleomagnetic and rock magnetic characteristics of the Upper Santonian sequences in the Aksu-Dere and Kudrino-2 sections, but at the same time have their own peculiarities.

The Kizil-Chigir and Chuku sections as well as the Upper Turonian–Coniacian part of the Aksu-Dere section exhibit a widely observed diamagnetic effect ($K < 0$, but the natural remanence is quite high, ranging from 0.1 to 1.5 × $10^{-3}$ A/m (except for outcrop 3176 in the Chuku section, where typical $\mathbf{J_n}$ values are as small as 0.005–0.05 × $10^{-3}$ A/m) (Figs. 3 and 4). The results of magnetic saturation and disintegration record a soft magnetic phase characteristic of fine-dispersed magnetite: saturation is achieved in the fields of 60–100 mT, the remanent coercive field ($\mathbf{B_{cr}}$) varies from 25 to 30 mT (Fig. 5a). The coercivity characteristics of the samples in the diagram are close to the segment of the predicted curve corresponding to pseudo single domain (PSD) magnetite (Dunlop, 2002) (Fig. 5b). The thermomagnetic analysis results are uninformative since in the heating curve, the peak corresponding to magnetite is nearly imperceptible, apparently due to extremely small $K$ values comparable to the instrumental error (Fig. 5c). The bend in the cooling curves at ~600°C (Fig. 5c) records a newly formed magnetite likely resulting from oxidation of iron reduced from organic matter or/and primary $Fe_3O_4$. The magnetic susceptibility anisotropy studies provide little information (Fig. 5d). The Turonian–Coniacian sequences of the Kizil-Chigir and Aksu-Dere sections as well as the Santonian part of the Chuku section are dominated by diamagnetic ricks. In samples with positive magnetic susceptibility, the distribution of the axes of magnetic ellipsoids is chaotic, which in most cases is likely due to the $K$ values being close to zero, comparable to the measurement error of the instrument.

The Turonian of the Kizil-Chigir section and the upper Turonian–Coniacian of the Aksu-Dere section are characterized by high paleomagnetic quality. These sediments are dominated by rocks with single component magnetization, which is ChRM with the maximum angular deviation (MAD) on the order of first degrees (Fig. 6).

In outcrops 3177, 3181, and 3175 in the Chuku section, two-component magnetization is more typical. The low-coercivity or low-temperature magnetization components are likely to be of a viscous origin (Fig. 6). ChRM quality is generally poorer than in other sections (MAD = 5°–15°), perhaps due to the small $\mathbf{J_n}$ values approaching the limit of measurement error of the instrument (Fig. 6).

In outcrop 3176 at Mt. Chuku, ChRM (as well as any other $\mathbf{J_n}$ components) could only be isolated at single levels (Fig. 3). In terms of their poor paleomagnetic quality, these rocks are similar to the Campanian deposits of the Aksu-Dere and Kudrino-2 sections (Guzhikov et al., 2021b).

Almost all paleomagnetic directions map on the lower hemisphere and cluster in the northern hemisphere, i.e., correspond to the normal polarity of the field (Figs. 3, 4, 7). The Aksu-Dere section (Upper Turonian, Coniacian, Upper Santonian) and outcrop 3177 of the Chuku section (lower(?)–upper Santonian) feature a very large scatter of paleomagnetic directions. The Kizil-Chigir (lower–middle Turonian) and Kudrino-2 sections as well as outcrops 3175 and 3181 of the Chuku section (upper Santonian) are characterized by higher ChRM concentration (Table 2, Fig. 7).

The components that differ from the section/outcrop mean paleomagnetic direction by more than 60° were preliminary interpreted as paleomagnetic anomalies and excluded from the statistical analysis of

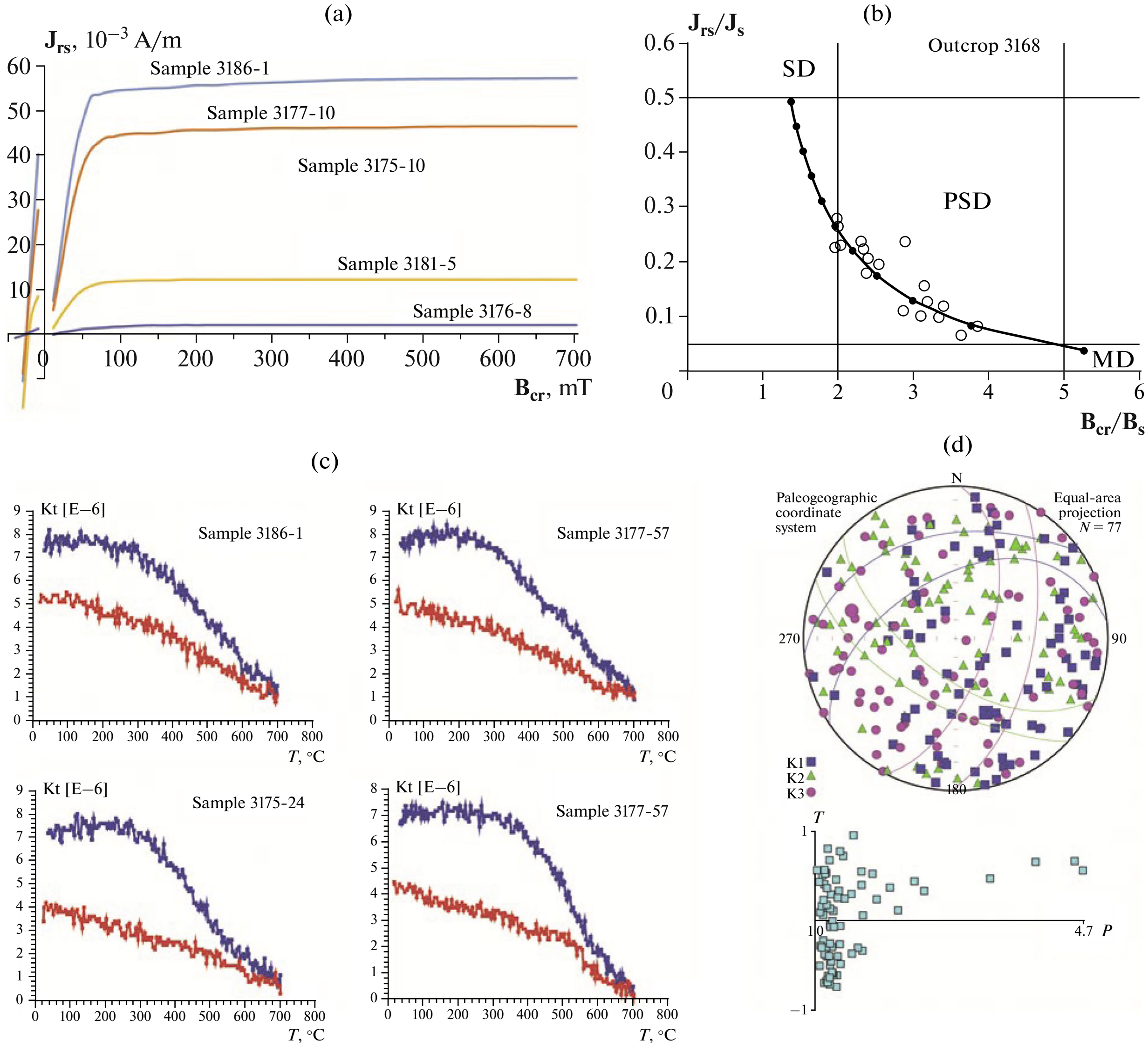


**Fig. 5.** Results of magnetic mineralogy studies: (a) magnetic saturation and disintegration curves; (b) Day diagram (SD, PSD and MD are single domain, pseudo single domain and multi domain regions, respectively); (c) thermomagnetic curves (red and blue for heating and cooling, respectively); (d) magnetic susceptibility anisotropy data: stereogram projections of maximum (K1), intermediate (K2), and minimum (K3) AMS axes with confidence ovals in paleogeographic coordinates, and *P*–*T* plots (*P* is anisotropy degree, *T*—factor positive and negative values indicate prolate and oblate ferromagnetic grains, respectively); *n* is number of specimens in sample.

ChRM (Table 2, Fig. 7). Overall, ten anomalies were revealed, sporadically scattered across the sections. The final conclusions concerning the number of excursions in the sections, based on the conversion results of directions into VGP, are summarized below in the Discussion section. Given the fact that anomalous directions are determined from one or two levels, while substantiating a microzone requires data from at least three consecutive levels, the microzones of anomalous polarity are shown half the thickness of the paleomagnetic column (Fig. 3, Fig. 4).

Within each studied outcrop except for 3180, the paleomagnetic concentrations in the geographic and stratigraphic coordinate systems ($k_g$ and $k_s$, respectively) are statistically indistinguishable (Table 2, Fig. 7). The fold test is inconclusive. The failure of the test is most likely to be due to two main factors. The first is insignificant differences in the bedding attitudes of the strata the paleomagnetic samples were taken from. In outcrop 3180, where bedding variations are significant, the testing results of the data from 12 samples taken from different limbs of the subaqueous slump fold (Fig. 2c, Fig. 7f) unambiguously indicate the post-folding age of ChRM at the level of significance $p = 0.01$. Meanwhile, the post-folding age is not necessarily related to the remagnetization of rocks. The

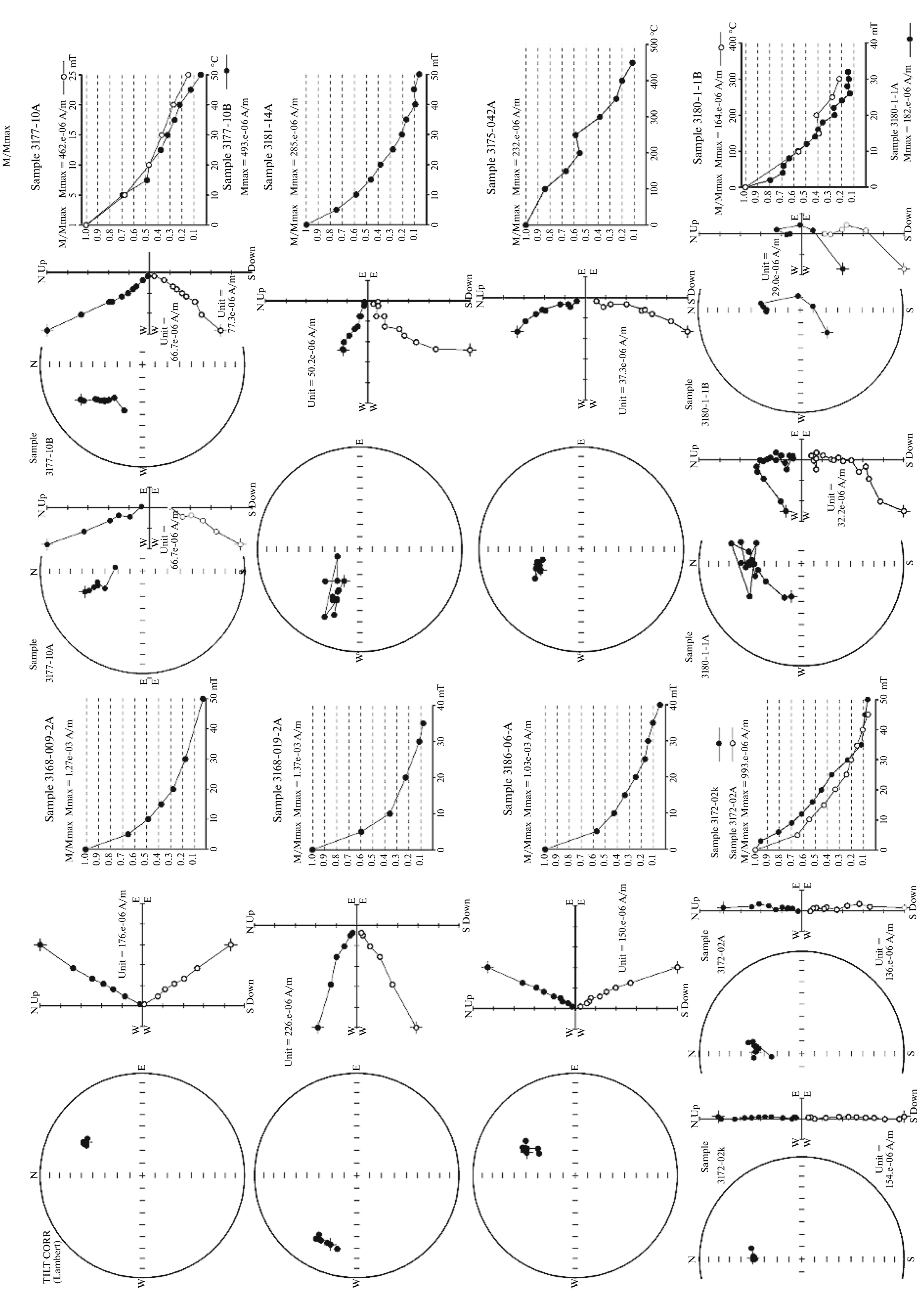

**Fig. 6.** Typical results of component analysis (polar stereographic projections, Zijderveld diagrams, demagnetization plots). Data are presented in stratigraphic coordinate system. *1*, *2*, *3* indicate $\mathbf{J}_n$ projections on lower hemisphere, on horizontal and vertical plane, respectively.

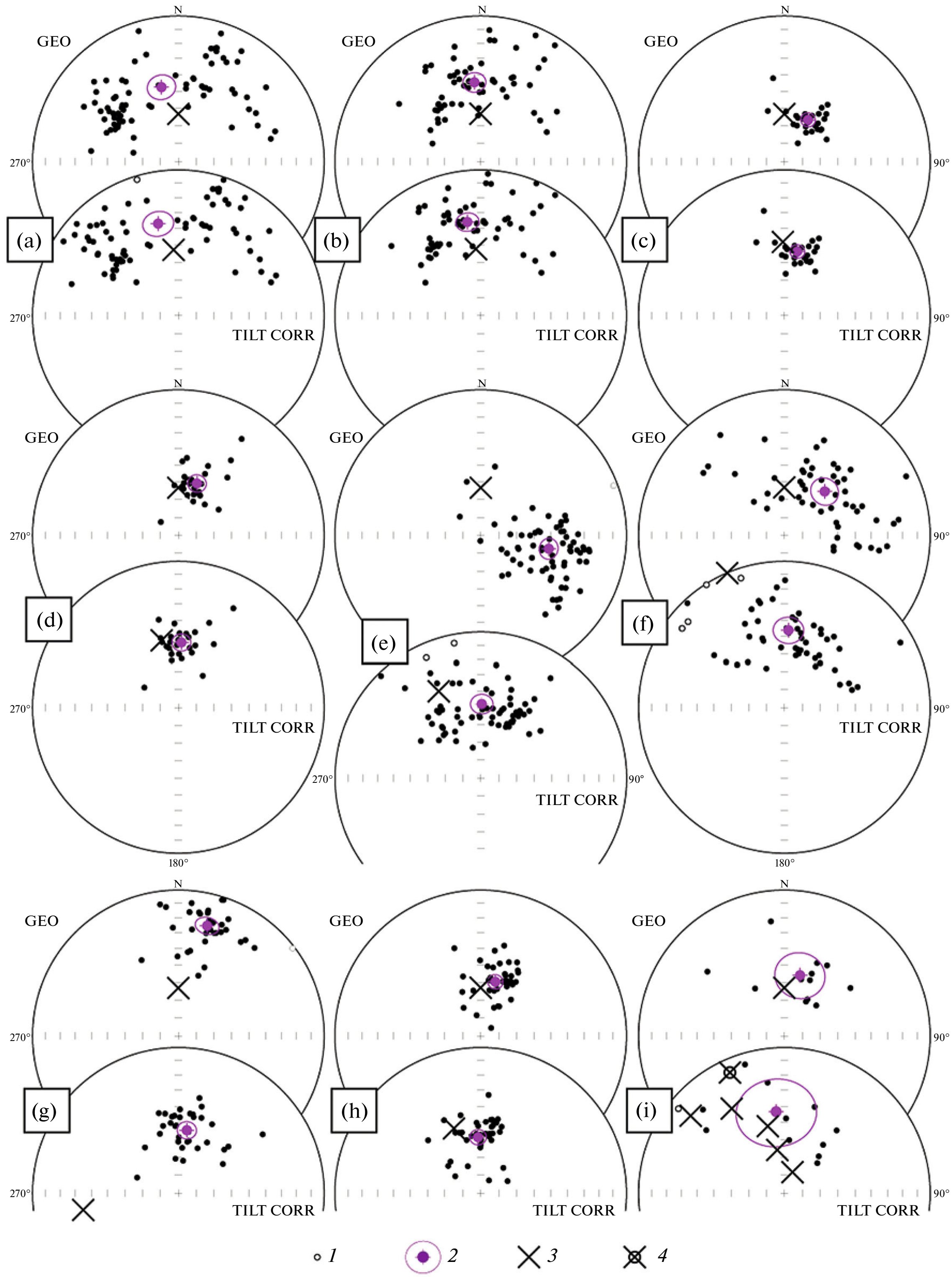


**Fig. 7.** ChRM polar stereographic projections for sections/outcrops in geographic (top) and stratigraphic (bottom) coordinate systems. (a), (b) Aksu-Dere section (outcrop 3168): (a) upper Turonian–Coniacian, (b) upper Santonian; (c) Kizil-Chigir section (outcrops 3186, 3172), lower–Middle Turonian; (d) Kudrino-2 (outcrop 3184), top upper Santonian; (e) Chuku section: outcrop 3177 (samples 1–47) (lower?)–upper Santonian; (f) outcrop 3177 (samples 48–78), upper Santonian; (g) outcrop 3181; (h) outcrop 3175; (i) outcrop 3180. *1*, ChRM upper hemisphere projections; *2*, projections of mean paleomagnetic directions with confidence circles ($\alpha_{95}$); *3*, *4*, lower and upper hemisphere projections of directions of remagnetization by present field, respectively. Other designations are same as in Fig. 6.

**Table 2.** Statistical parameters of distributions of ChRM and virtual geomagnetic poles (VGP)

| Figure | Sections (outcrops), age | $n/N$ | | D, deg | I, deg | $k$ | $\alpha_{95}$, deg | $F$, deg | $L$, deg | $f_m$, deg | $A_{95}$, deg |
|---|---|---|---|---|---|---|---|---|---|---|---|
| 7a | Aksu-Dere (3168, samples 1–20A), late Turonian–Coniacian | 74 | Geo | 347.2 | 46.4 | 6.02 | 7.4 | | | | |
| | | | Tilt | 347.6 | 35.6 | 5.56 | 7.7 | 63.0 | 240.4 | 19.7 | 8.7 |
| 7b | Aksu-Dere (3168, samples 21–40), late Santonian | 60 | Geo | 355.5 | 44.5 | 10.71 | 5.9 | | | | |
| | | | Tilt | 351.9 | 35.4 | 11.18 | 5.7 | 63.9 | 231.5 | 19.5 | 7.1 |
| | Aksu-Dere (3168), Late Turonian–Coniacian, late Santonian | 134 | Geo | 351.1 | 45.6 | 7.47 | 4.8 | | | | |
| | | | Tilt | 349.7 | 35.5 | 7.20 | 4.9 | 63.5 | 236.3 | 19.6 | 8.1 |
| 7c | Kizil-Chigir (3172, 3186), early–middle (–late?) Turonian | 26 | Geo | 29.5 | 63.0 | 52.19 | 4.0 | | | | |
| | | | Tilt | 11.4 | 52.9 | 52.21 | 4.0 | 75.8 | 187.9 | 33.5 | 5.1 |
| 7d | Kudrino-2 (3184), top of late Santonian | 26 | Geo | 19.6 | 58.9 | 32.57 | 5.0 | | | | |
| | | | Tilt | 2.6 | 53.4 | 33.2 | 5.0 | 79.1 | 202.4 | 33.9 | 5.8 |
| 7e | Chuku (3177, samples 1–47), (early?)–late Santonian | 69 | Geo | 102.1 | 50.0 | 12.14 | 4.9 | | | | |
| | | | Tilt | 1.1 | 48.7 | 10.79 | 5.4 | 74.9 | 210.3 | 29.7 | 7.4 |
| 7f | Chuku (3177, samples 48–78), late Santonian | 53 | Geo | 42.6 | 56.4 | 7.48 | 7.7 | | | | |
| | | | Tilt | 3.1 | 46.1 | 7.11 | 7.9 | 72.6 | 204.9 | 27.5 | 8.1 |
| 7g | Chuku (3181), late Santonian | 35 | Geo | 14.7 | 23.0 | 19.73 | 5.6 | | | | |
| | | | Tilt | 7.7 | 54.1 | 23.72 | 5.1 | 78.3 | 181.0 | 34.6 | 6.5 |
| 7h | Chuku (3175), late Santonian | 39 | Geo | 16.2 | 57.8 | 35.47 | 3.9 | | | | |
| | | | Tilt | 358.5 | 57.8 | 30.60 | 4.2 | 83.6 | 224.6 | 38.4 | 6.3 |
| 7i | Chuku (3180), late Santonian | 12 | Geo | 14.5 | 54.7 | 11.50 | 13.4 | | | | |
| | | | Tilt | 354.3 | 43.1 | 5.39 | 20.6 | | | | |
| 9a, b | Mean ChRM: All sections/outcrops | 7 | Geo | 27.1 | 55.4 | 10.6 | 19.4 | | | | |
| | | | Tilt | 1.9 | 49.6 | 83.7 | 6.6 | 75.7 | 207.4 | 30.4 | 4.3 |
| | Mean ChRM: without Aksu-Dere section | 6 | Geo | 34.7 | 55.8 | 10.9 | 21.3 | | | | |
| | | | Tilt | 4.6 | 51.7 | 218.6 | 4.5 | 77.1 | 196.3 | 32.4 | 3.6 |
| | | | | VGP for Stable Europe (Besse and Courtillot, 2022) | | 80 ± 10 Ma | | 81.4 | 206.1 | | 5.9 |
| | | | | | | 90 ± 10 Ma | | 82.2 | 202.1 | | 5.2 |
| | | | | | | 80 ± 5 Ma | | 81.0 | 232.5 | | 6.9 |
| | | | | | | 85 ± 5 Ma | | 81.1 | 230.5 | | 10.3 |
| | | | | | | 90 ± 5 Ma | | 80.8 | 185.8 | | 3.5 |
| | | | | | | 95 ± 5 Ma | | 81.8 | 183.4 | | 6.4 |

$n$ is number of samples; $N$ is number of sites (sections or/and outcrops); ChRM: D, I are mean paleomagnetic inclination and declination, respectively; $k$ is concentration parameter; $\alpha_{95}$ is radius of confidence circle of a vector; VGP: F is latitude, L is longitude, $f_m$ is paleomagnetic latitude, $A_{95}$ is confidence circle radius. Geo and Tilt are geographic and stratigraphic coordinate systems, respectively.

origin of the fold in outcrop 3180 allows the formation of $\mathbf{J_n}$ after the completion of deformation of the plastic sediment but before the end of its lithification. For the Upper Cretaceous sediments whose age is ~80–90 Ma, the substantiation of post-depositional (diagenetic) origin of ChRM is practically identical to the proof of its primary nature.

The second factor is the presence of layers with both pre-deformational (depositional or post-depositional) and post-deformational (post-depositional) magnetization in one section (outcrop). Theoretically, the magnetization in strata subjected to landslide deformations at the stage of diagenesis can be a stabilized vector sum of the pre- and post-deformational magnetization components. This phenomenon could explain the anomalous scatter of ChRM without linking it to the changes in the geomagnetic field vector. Obviously, in the analysis of the total magnetization components (Fig. 8a), the performance of the fold test will be greatly reduced, up to the point of no clear result. However, in this case, the effect of distortion of the true paleomagnetic direction due to the summation of the pre- and post-deformational components should increase with the increase in the dip angles of the beds, whereas in reality, this a trend is not observed (Fig. 8b). No significant correlation between the distortion of the paleomagnetic vector and the dip angle of the bed is revealed, irrespective of whether the analysis is conducted for the entire data or for each section separately. Therefore, the hypothetical summation of different components of $\mathbf{J_n}$, which cannot be separated during demagnetization processing, cannot be the primary cause of ChRM variations in the sediments under study.

The age of magnetization relative to the neotectonic stage, which determined the present-day structural geometry, is established due to the significant difference in the bedding of strata in different regions of the southwestern Crimea. The observed distributions of the section-mean ChRMs have a large scatter in the geographic and high concentration in the stratigraphic coordinate systems: $k_s$ is a factor of 7.9 higher than $k_g$ (if we exclude the Aksu-Dere section (outcrop 3168), where the mean direction statistically differs from the mean paleomagnetic vectors in other sections, then $k_s/k_g = 20.1$) (Fig. 9, Table 2). The F-test of the concentration ratios gives their significance at $p = 0.01$, which alone proves the pre-folding age of the magnetization (Shipunov, 1995). The results of the fold test support the pre-folding age of ChRM at the significance level $p = 0.01$ when testing the data both over the entire set of the sections and after excluding the Aksu-Dere section (the mean bedding attitudes for each section/outcrop were calculated from the average ChRM in the geographic and stratigraphic coordinate system). Thus, the results of the fold test reject remagnetization of rocks at the neotectonic stage and are consistent with the hypothesis of the post-depositional (diagenetic) nature of magnetization.

From the observations in the Kizil-Chigir (Turonian) and Kudrino-2 sections and outcrops 3175, 3181 of the Chuku section (upper Santonian), where the paleomagnetic concentrations are fairly high (>30), we calculated the average virtual geomagnetic poles (VGP), which are statistically indistinguishable from the 80–95 Ma VGP determined for stable Europe, corresponding to the Turonian–Santonian (Gradstein et al., 2020) (Table 2). This provides additional evidence for the ancient nature of the magnetization.

The obtained data meet at least seven out of eight criteria prescribed for assessing the reliability of magnetostratigraphic materials in the Stratigraphic Code of Russia (Khramov and Shkatova, 2000), and six out of seven criteria for assessing the quality of paleomagnetic data proposed by Van der Voo (1990). This allows the obtained results to be used in stratigraphic correlations and geodynamic reconstructions. The variations in ChRM in this case do not claim an accurate record of the fine structure of the field in the sections, due to the uncertain time of acquisition of post-depositional magnetization (Pechersky, 2010), but unambiguously indicate the very fact of the presence of high-amplitude paleosecular variation in the studied stratigraphic interval.

## DISCUSSION

Based on the existing biostratigraphic data, the graphs of variations in the deviation of the VGP, calculated at each stratigraphic level, from the section/outcrop mean VGP were correlated to the geologic time scale (Gradstein et al., 2020) (Fig. 10). Following the definition of a paleomagnetic excursion as a deviation of a pole from its mean position by 45° or more (Jacobs, 2007), in the composite paleomagnetic column, in addition to the ten anomalies detected by the ChRM analysis, 18 other anomalies should be included. A single excursion is detected in the Turonian. Eight excursions are confined to the Coniacian, and two of them, based on the samples from three and five consecutive levels, respectively, correspond to the full-scale magnetostratigraphic units—microzones of anomalous polarity $A_1k$ and $A_2k$. Fifteen out of 19 levels in the Santonian, in which the excursions are identified, are grouped into one large microzone of anomalous polarity $A_1st$. All the Coniacian excursions are characterized by the deviations of 45° to 63°, and most Santonian excursions have deviations ranging between 90° and 150° (Fig. 10).

To approximately estimate the amplitude of the paleosecular variation, we used the simplest but effective parameter—standard deviation S (formula (1)) with a fixed cutoff angle of 45° (McElhinny and McFadden, 1997).

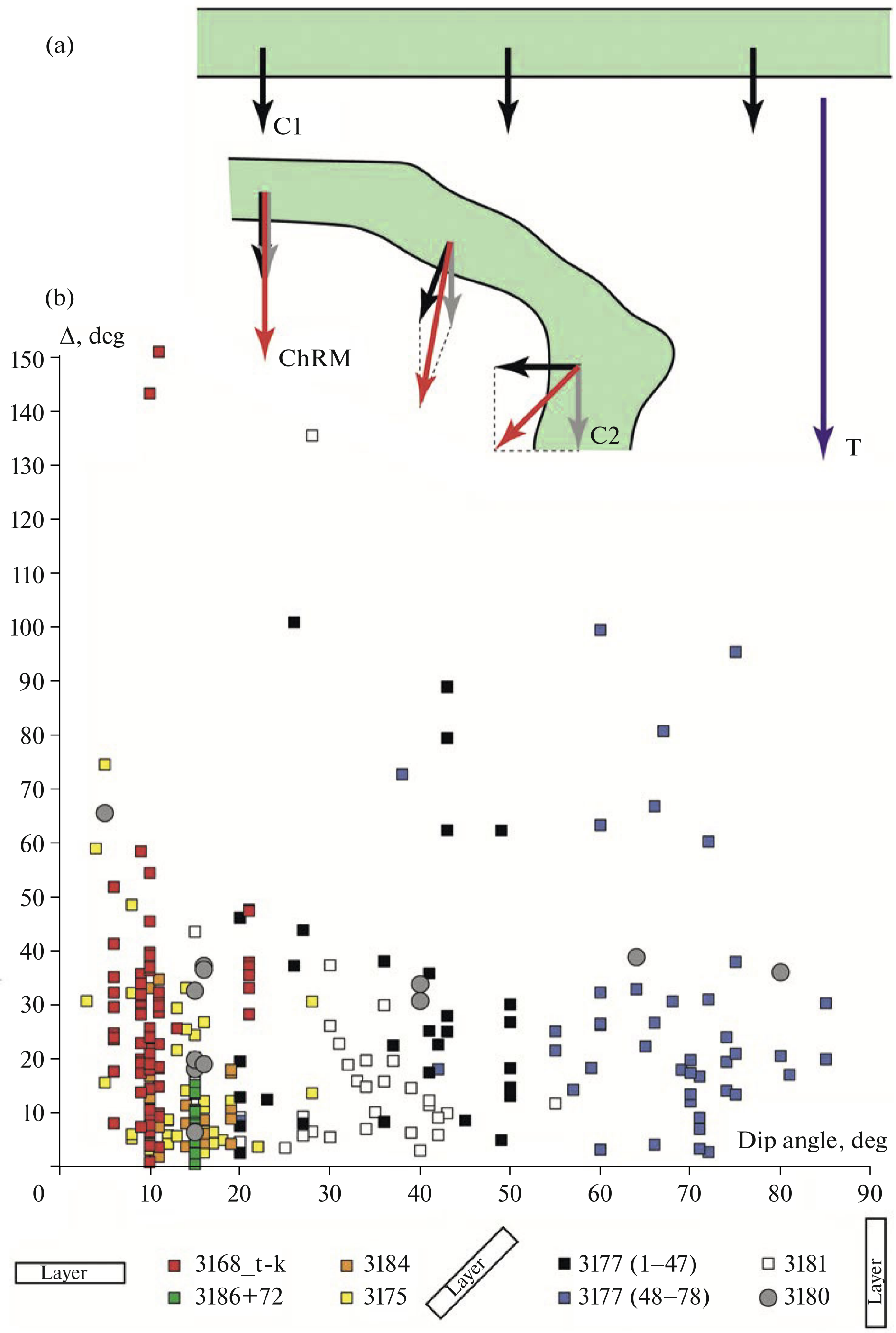


**Fig. 8.** (a) Schematic illustration of hypothetical dependence of scatter in paleomagnetic vectors on layer deformation intensity in subaqueous slump fold provided that ChRM is a stabilized vector sum of pre- (C1) and post-deformation (C2) magnetization components and that geomagnetic field vector (**T**) is unchanged; (b) diagram illustrating empirical relationship between angle Δ, which is formed by ChRM at each level with section/outcrop mean ChRM), and dip angle of a layer.

The amplitude of the deviations is minimal in the early–middle Turonian, reaches a maximum in the late Turonian–Coniacian, decreases slightly in the early(?)–late Santonian, and drops to a minimum by the very end of the Santonian (Table 3). The Santonian–Campanian boundary layers (top of outcrop 3175 in the Chuku section) recorded an increase in the amplitude of the Paleocene variations, probably

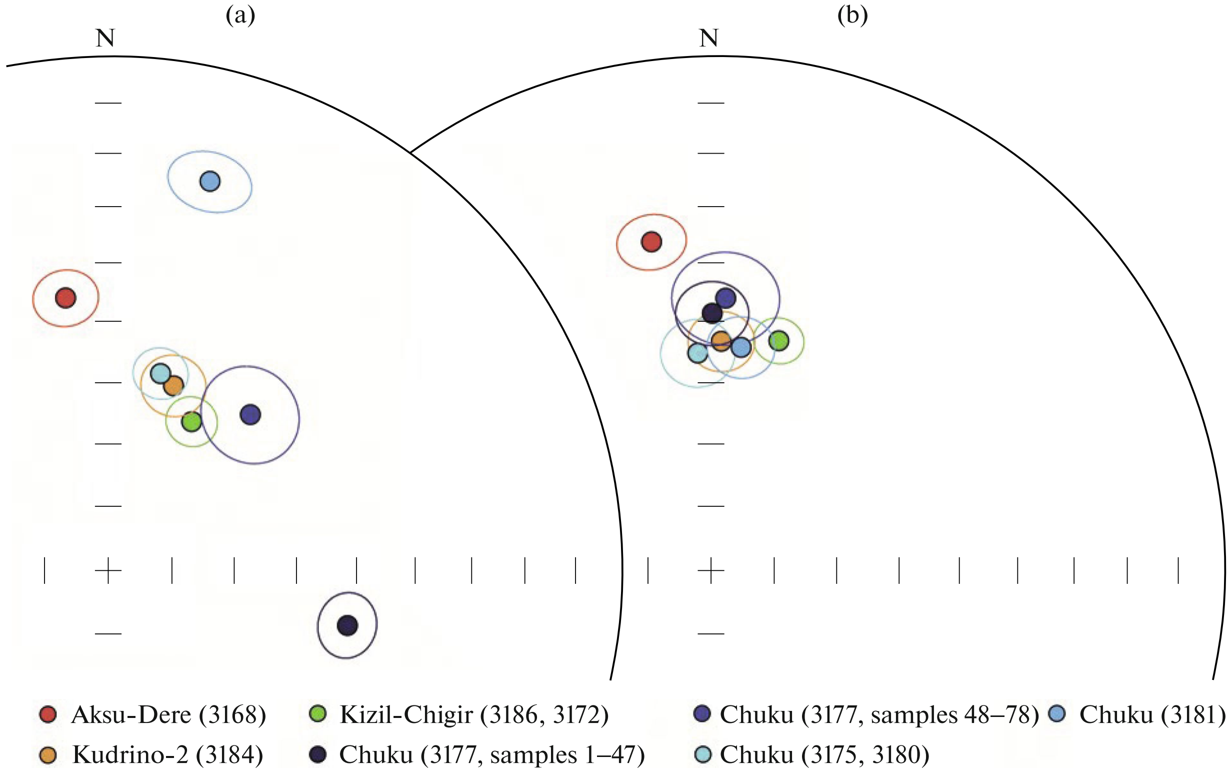


**Fig. 9.** Polar stereographic projections with site (section/outcrop) mean ChRM in (a) geographic and (b) stratigraphic coordinate systems.

related to the beginning of the reversal from Chron 34n to Chron 33r. The results of the BF analysis suggest that in the Kudrino-2 reference section which documented the base of Chron 33r (Guzhikov et al., 2021b), the age analogs of the top strata of outcrop 3175 can be reduced.

The obtained $S_{45}$ values in the early–middle Turonian and late Santonian (from 11.5° to 15.6°) are fairly consistent with the model latitudinal dependences of paleosecular variation for the Cretaceous Normal Superchron (Lebedev et al., 2022), and in the late Turonian, Coniacian, and Santonian they reach 31.1°, approximately double the model predictions (~12°–16°).

The maximum amplitude of variations is observed in the late Turonian–Coniacian, but the number and amplitude of the excursions regularly increase from the Turonian to the Santonian (Fig. 10). Therefore, in this case, the amplitude $S$ calculated from all poles without exception (Table 3) is a useful parameter quantifying the changes in the degree of "anomalousness" in the behavior of the geomagnetic field.

The same regularities in the pattern of paleosecular variation and excursions during the Turonian–Santonian are more clearly expressed in the VGP trajectories calculated for different time slices (Fig. 11). The paths of the coeval VGPs determined from the data from the remote sections (the distance between the Chuku section and the Aksu-Dere and Kudrino-2 sections is ~10 km) are similar both in the amplitude of the variations (variances are statistically indistinguishable) and in their positions on the Earth's surface (Figs. 11c, 11g, 11d).

The close similarity, up to the details, of the coeval VGP trajectories in the remote sections, along with the regular character of variations in $S$ across the composite section, are the main arguments in favor of the idea that the studied rock sequence documents the fine structure of the Turonian–Santonian geomagnetic field.

The mere detection of a record of secular variation with anomalously high amplitude in sediments is not uncommon. Such behavior of the field is characteristic of the epochs of geomagnetic reversals or excursions. If reliable biostratigraphic data were not available, in such a situation the most likely conclusion would be that the studied sediments were formed over a short period of time, because according to modern concepts, the reversals are rapid events which take less than 20 kyr to occur (Valet and Herrero-Bervera, 2007). However, in the discussed case, we studied the reference sections with reliable paleontological evidence, which leaves no doubt about the stratigraphic completeness of the upper Turonian, Coniacian, and

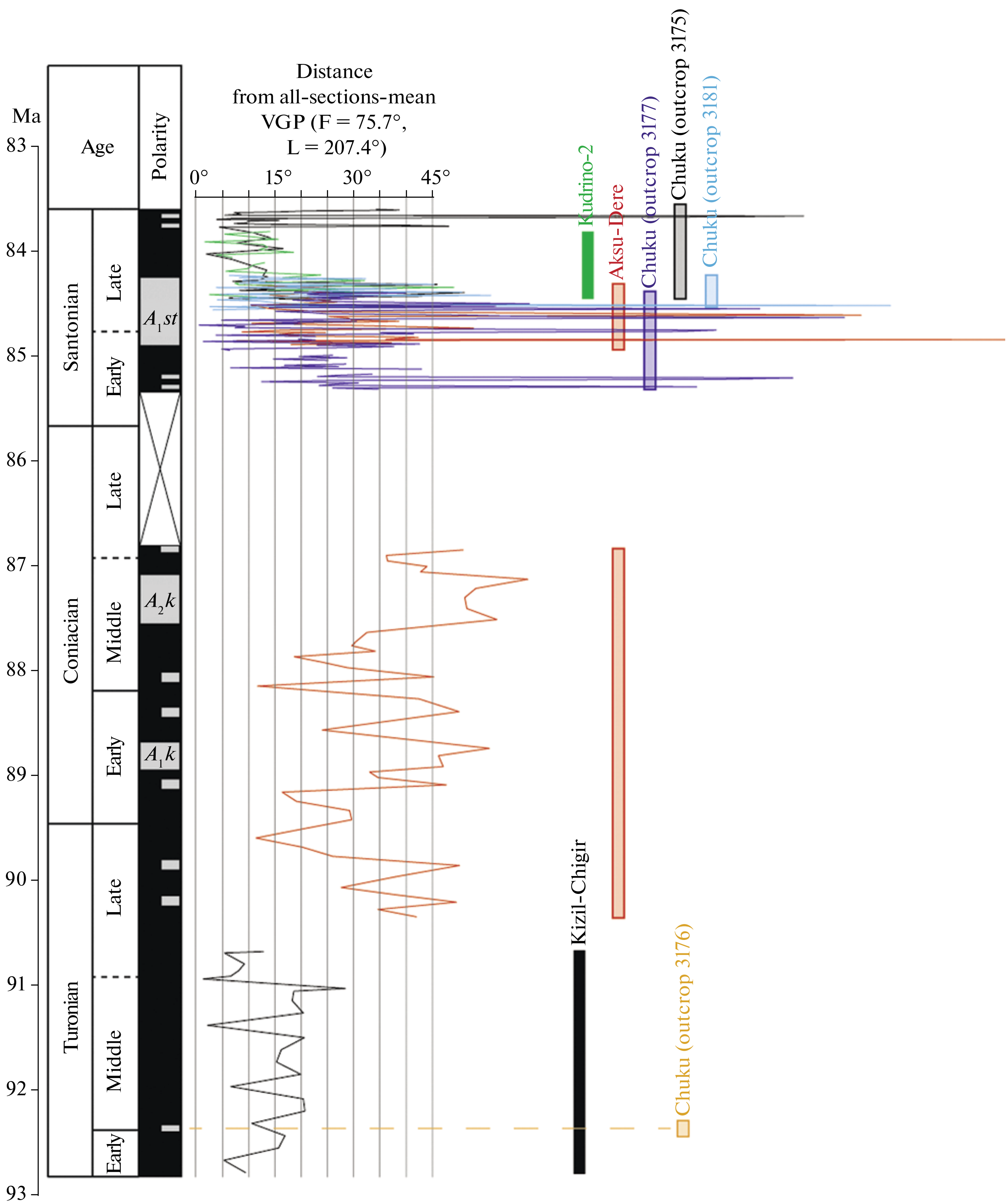


**Fig. 10.** Schematic composite magnetochronologic section of Santonian–Turonian in southwestern Crimea. Designations are same as in Fig. 3. For outcrop 3176, only Turonian part is shown.

lower(?)–upper Santonian sequences which were formed over a period of ~6 Myr (Gradstein et al., 2020). Therefore, the obtained data indicate an anomalous behavior of the geomagnetic field, peculiar to the epochs of geomagnetic reversals or excursions, but existing for several million years.

**Table 3.** Paleosecular variation amplitude estimates

<table>
<tr><th>Figure</th><th>Section (outcrop)</th><th>N / n</th><th>S, deg</th><th>S<sub>45</sub>, deg</th><th>S, deg</th><th>S<sub>45</sub>, deg</th><th>S, deg</th><th>S<sub>45</sub>, deg</th></tr>
<tr><td>11a</td><td>Kizil-Chigir (3186, 3172)</td><td>23/23</td><td>15.6 [12.1; 22.1]</td><td>15.6 [12.1; 22.1]</td><td></td><td></td><td></td><td></td></tr>
<tr><td>11b</td><td>Aksu-Dere (3168, samples 1–20A)</td><td>39/26</td><td>39.4 [32.2; 50.8]</td><td>31.1 [24.4; 42.9]</td><td></td><td></td><td rowspan="3">42.1 [37.7; 47.6]</td><td rowspan="3">25.9 [23.0; 29.7]</td></tr>
<tr><td>11c</td><td>Aksu-Dere (3168, samples 21–40)</td><td>32/28</td><td>45.1 [36.2; 60.0]</td><td>25.9 [20.5; 35.3]</td><td rowspan="2">43.0 [37.9; 49.8]</td><td rowspan="2">24.4 [21.3; 28.6]</td></tr>
<tr><td>11c</td><td>Chuku (3177)</td><td>73/63</td><td>42.7 [36.7; 51.0]</td><td>26.0 [22.1; 31.5]</td></tr>
<tr><td>11d</td><td>Chuku (3175, samples 1–9)</td><td>9/7</td><td>33.7 [22.8;64.6]</td><td>26.9 [17.3; 59.2]</td><td></td><td></td><td rowspan="3">30.0 [25.2; 37.0]</td><td rowspan="3">18.3 [15.2; 23.0]</td></tr>
<tr><td>11d</td><td>Kudrino-2 (3184, samples 1B–10)</td><td>13/12</td><td>22.2 [15.9;36.6]</td><td>17.9 [12.7; 30.4]</td><td rowspan="2">29.3 [24.3; 37.0]</td><td rowspan="2">16.7 [13.7; 21.4]</td></tr>
<tr><td>11d</td><td>Chuku (3181)</td><td>32/28</td><td>32.5 [26.1; 43.2]</td><td>16.8 [13.3; 22.9]</td></tr>
<tr><td>11e</td><td>Kudrino-2 (3184, samples 11–24)</td><td>13/13</td><td>12.2 [8.7; 20.1]</td><td>12.2 [8.7; 20.1]</td><td rowspan="2">11.6 [9.1; 15.9]</td><td rowspan="2">11.6 [9.1; 15.9]</td><td></td><td></td></tr>
<tr><td>11e</td><td>Chuku (3175, samples 10–24)</td><td>14/14</td><td>11.5 [8.3; 18.5]</td><td>11.5 [8.3; 18.5]</td><td></td><td></td></tr>
<tr><td>11f</td><td>Chuku (3175, samples 25–45)</td><td>18/16</td><td>42.7 [32.0; 64.0]</td><td>20.8 [15.4; 32.2]</td><td></td><td></td><td></td><td></td></tr>
</table>

*N* is number of VGPs used in estimation of variation amplitude (*S*) without rejection (coincides with number of levels from which paleodeterminations including excursions are obtained); *n* is number of VGPs used in estimation of variation amplitude with cutoff angle 45° ($S_{45}$). Figures in square brackets indicate lower and upper limits of 95% confidence intervals for estimates of *S*.

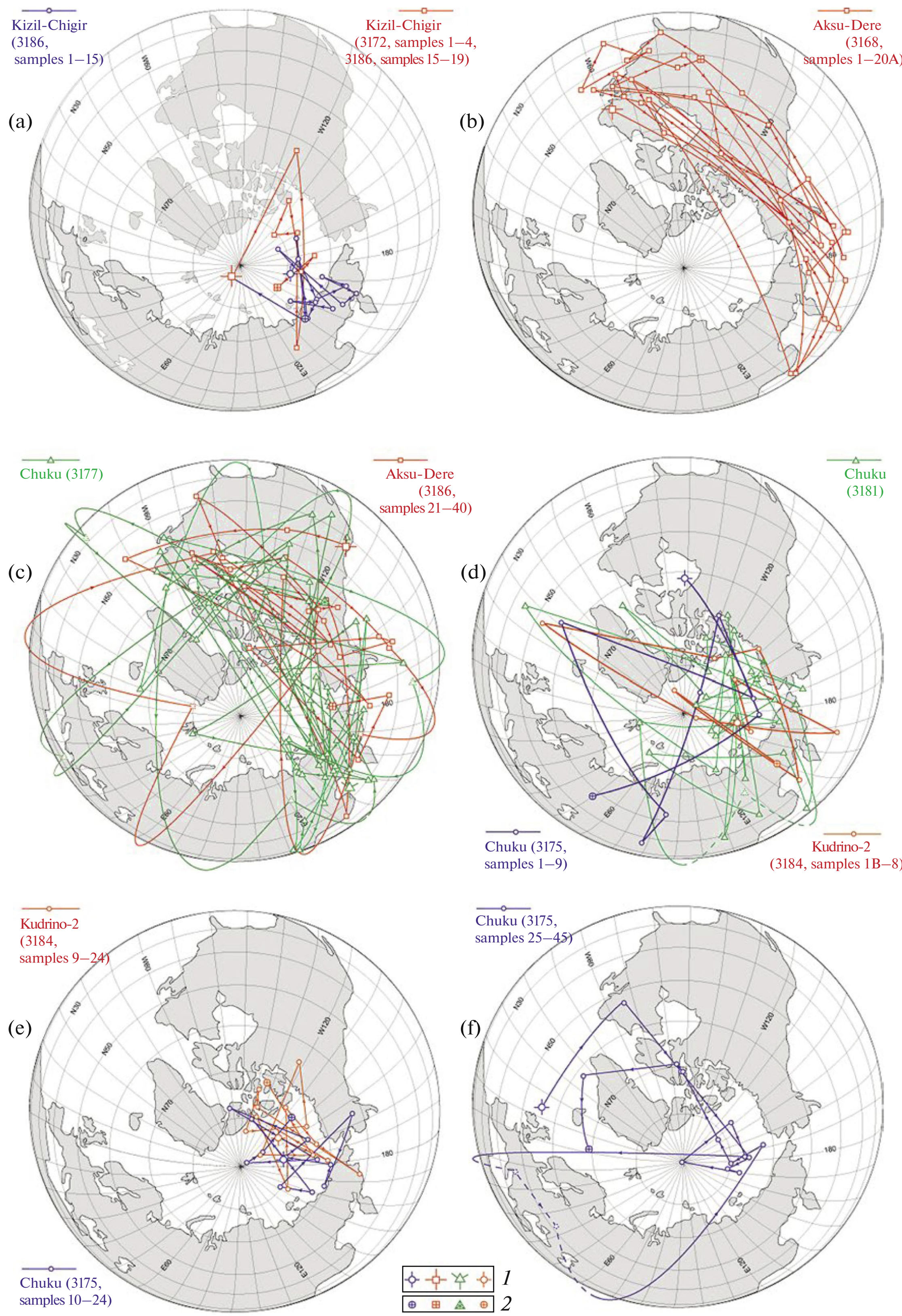


**Fig. 11.** VGP trajectories for different age slices: (a) early–middle Turonian; (b) late Turonian–Coniacian; (c) early(?)–late Santonian; (d) late Santonian; (e) end of late Santonian; (f) Santonian–Campanian boundary interval. *1* and *2* are start and end points of VGP trajectories.

The results for the Southwestern Crimea agree well with the independent data on the intricate paleomagnetic zonality of the Turonian, Coniacian, and Santonian in Tuarkyr, Turkmenistan (Guzhikova et al, 2003), Lower–Middle Volga region (Guzhikova et al., 2020; 2021; 2019), West Siberia (Gnibidenko et al., 2014), Southern England (Montgomery et al., 1998), and other regions (Eremin et al., 1995; Fomin and Eremin, 1993). A common feature of the Turonian–Santonian paleomagnetic columns in remote sections is the presence of numerous magnetozones of anomalous and/or reversed polarity against the background of dominant normal polarity in the Turonian–Coniacian and prevailing reversed (anomalous) polarity in the Santonian. The differences in the details of paleomagnetic structure in the sections of coeval sediments in remote regions are quite natural if we assume that the dipole pattern of the geomagnetic field was often disrupted in the Turonian–Santonian.

Some authors, e.g., Gale et al. (2023) are skeptical about the reliability of the magnetostratigraphic data that testify to the complex paleomagnetic zonation of the Turonian–Santonian. However, the reliability of magnetostratigraphic material for any particular section may be subject to justified criticism. Therefore, to establish the true character of the geomagnetic field, the decisive criterion is still the so-called external convergence test, which involves tracing an identical paleomagnetic structure in sediments of the same age in different regions.

Of all the the data on ancient sedimentary rocks available to us, the longest period of anomalous geomagnetic field state (~110 ka according to cyclostratigraphic estimate) was recorded in the Permian–Triassic boundary interval of the Russian Plate (Fetisova et al., 2022). Records of the fine structure of igneous rocks are limited by the time of their formation, which is very short in terms of geologic time scales. However, along with the lack of reliable information on the anomalous state of the field during a long period of time (on the order of millions of years), we also note the paucity of reliable paleomagnetic data testifying to stable normal polarity conditions in the Turonian, Coniacian, and Santonian. The notions about the monopolar structure of the Cretaceous superchron are mainly based on the calibration results of the linear magnetic anomalies (LMA) sequence with magnetostratigraphic data for the Upper Cretaceous of the Northern Mediterranean, mainly Italy. Meanwhile, neither the LMA, whose isolation in the ancient (Mesozoic) oceanic crust is problematic, nor the Upper Cretaceous sections in Italy, whose postulated exceptional stratigraphic completeness is questionable, can be recognized as the main sources of information for the construction of the geomagnetic polarity scale (Guzhikova et al., 2007; 2019). Therefore, the data on the Turonian–Santonian of the Crimea, which are highly competitive in the quality of the paleomagnetic material with their age analogs in Italy, are a valid incentive to revise the traditional views of the geomagnetic field behavior at the end of the Cretaceous superchron.

The hypothesis about the anomalous behavior of the Turonian–Santonian field is indirectly confirmed by paleointensity determinations from effusive rocks of Transcaucasia, which suggest that the intensity of the Coniacian–Santonian geomagnetic field decreased to one fifth to one tenth of the modern value (Solodovnikov, 2001). However, according to the summary presented in (Kurazhkovskii et al., 2022), both low and high paleointensities occurred in each age. From this standpoint, the Turonian, Coniacian, and Santonian ages (~95–85 Ma) do not fundamentally differ from other time intervals in the last 170 Ma.

The revealed features of the fine structure of the field are most likely averaged over a period on the order of hundreds of thousands to millions of years. This is unambiguously indicated by the statistically indistinguishable coordinates of the Santonian average paleomagnetic poles both from outcrops 3177-A, 3177-B on Mt. Chuku where the most intense paleointensity variations were recorded, and from outcrops 3175 and 3181 on Mt. Chuku and the Kudrino-2 section, where the amplitude of variations is much lower (Table 2). The time of sediment formation in the Chuku section can be estimated from the average duration of benthic foraminifera zones calculated by dividing the duration of the age by the number of BF zones in the stage (an order of hundreds of thousands of years). No statistically significant differences are also observed in the positions of the mean VGPs from the upper Turonian–Coniacian and upper Santonian of the Aksu-Dere section. The time required for the formation of upper Turonian–Coniacian (~3–4 Myr) and upper Santonian sediments (~1–2 Myr) in the Aksu-Dere section is estimated owing zonal division not only in benthic, but also in planktonic foraminifers and nannoplankton (Guzhikov et al., 2021a; 2021b; Guzhikova et al., 2020; Kopaevich and Valaschik, 1993; Scherbinina and Gavrilov, 2016). The PF and nannoplankton zones are correlated, with a share of convention, to the absolute age in the Geologic Time Scale (Gradstein et al., 2020).

The mean pole over the studied sections, except for Aksu-Dere, statistically coincides with the Turonian–Santonian poles calculated for stable Europe (Besse and Courtillot, 2002) (Table 2), thus supporting the view that the Mountainous Crimea docked with the southern margin of Eurasia approximately in the middle of the Cretaceous (Pechersky and Safonov, 1993).

In order for the average pole over the Aksu-Dere section to coincide with the average pole over the other sections, when converting the average paleomagnetic vector of the Aksu-Dere section from the geographic to the stratigraphic coordinate system, we have to introduce a correction for a bed with a dip azimuth of 115° and dip angle 13°. In principle, these attitude elements may correspond to the plane of an undetected local fault along which the rock block underwent a displacement accompanied by a gentle tilting and eastward turning. The discussion of the validity of this assumption requires multifaceted geological information and, in any case, is beyond the scope of this work. However, the proposed hypothesis illustrates practical potential of paleomagnetic data for refining the structure and geodynamics of the southwestern Crimea.

## CONCLUSIONS

High-quality paleomagnetic data documenting the record of the Paleocene variations of anomalously large amplitude and numerous geomagnetic excursions have been obtained from the Turonian, Coniacian, and Santonian reference sections in the southwestern Crimea. The anomalous state of the geomagnetic field, characteristic of transitional epochs, dominated for ~6 Myr (late Turonian–Santonian). The stratigraphic completeness of the sections is controlled by the biostratigraphic data, which rules out the idea that the fine structure of the field was recorded over a short period of time.

The paleomagnetic data for the Turonian–Santonian of the SW Crimea are fundamentally consistent with the material for the coeval deposits of southern England (Montgomery et al., 1998), the Volga region (Guzhikova, 2020; 2021; Guzhikova et al., 2019), Tuarkyr (Guzhikov et al, 2003), Western Siberia (Gnibidenko et al., 2014), and other regions that document the complex (alternating or anomalous) paleomagnetic zonation of the Turonian, Coniacian, and Santonian stages. Consdidered collectively, this information provides the possibility of revisiting the existing notions about normal regime of the geomagnetic field at the end of the Cretaceous superchron, given that the alternative data suggesting a simple monopolar structure of the Turonian–Santonian field are limited and inconclusive.

## ACKNOWLEDGEMENTS

We are grateful to A.G. Manikin and V.A. Grishchenko (Saratov State University), E.V. Naumov and D.S. Bolotova (Moscow State University) for their participation in the field studies of the sections. We thank A.O. Safonova, D.A. Agibalov, and R.A. Tuyakov (Saratov State University) for their assistance in the laboratory studies. We acknowledge N.E. Mikhaltsov (Trofimuk Institute of Petroleum Geology and Geophysics of the Siberian Branch of the Russian Academy of Sciences, Novosibirsk) for conducting thermomagnetic analysis. We are indebted to V.E. Pavlov, R.V. Veselovskiy, G.P. Markov, and other members of the Laboratory of the Main Geomagnetic Field and Rock Magnetism of the Schmidt Institute of Physics of the Earth of the Russian Academy of Sciences for providing the possibility of conducting measurements on cryogenic magnetometer. We are also grateful to D.K. Nurgaliev and D.M. Kuzina (Kazan Federal University) and A.M. Surinskii (Saratov State University) for their assistance in the work with the coercimeter.

## FUNDING

The study was supported by the Russian Science Foundation under project no. 22-17-00091, https://rscf.ru/project/22-17-00091/.

## CONFLICT OF INTEREST

The authors of this work declare that they have no conflicts of interest.

## REFERENCES

AGICO, Anisoft: Advanced Treatment of Magnetic Anisotropy Data. https://www.agico.com/text/software/anisoft/anisoft.php. Cited April 7, 2023.

Alekseev, A.S., Upper Cretaceous, in *Geologicheskoe stroenie Kachinskogo podnyatiya Gornogo Kryma. Stratigrafiya mezozoya* (Geological Structure of the Kachin Uplift of the Crimean Mountains. Mesozoic Stratigraphy), Mazarovich, O.A. and Mileev, V.S., Eds., Moscow: MGU, 1989, pp. 123–157.

*Atlas melovoi fauny Yugo-Zapadnogo Kryma* (Atlas of the Cretaceous Fauna of South-Western Crimea), Arkad'ev, V.V. and Bogdanova, T.N., Eds., St. Petersburg: Pangeya, 1997.

Baraboshkin, E.Yu., Arkadiev, V.V., and Kopaevich, L.F., Reference sections of the Cretaceous system of Mountainous Crimea. Guidebook of the field excursions, *Materialy VIII Vserossiiskogo soveshchaniya, 26.09–3.10.2016* (Proc. VIII All-Russ. Meeting, September 26–October 3, 2016), Baraboshkin, E.Yu., Ed., Simferopol: ChernomorPRESS, 2016.

Baraboshkin, E.Yu., Guzhikov, A.Yu., Aleksandrova, G.N., Fomin, V.A., Pokrovskii, B.G., Grishchenko, V.A., Manikin, A.G., and Naumov, E.V., New sedimentological, magnetostratigraphic, and biostratigraphic data on the Campanian–Maastrichtian of Beshkosh Mountain, Southwest Crimea, *Stratigr. Geol. Correl.*, 2020, vol. 28, no. 6, pp. 816–858.
https://doi.org/10.1134/S0869593820060040

Beniamovsky, V.N., Infrazonal biostratigraphy of the Upper Cretaceous in the East European province based on benthic foraminifers, Part 1: Cenomanian-Coniacian, *Stratigr. Geol. Correl.*, 2008, vol. 16, no. 3, pp. 257–266.

Besse, J. and Courtillot, V., Apparent and true polar wander and the geometry of the geomagnetic field over the last 200 Myr, *J. Geophys. Res.: Solid Earth,* 2002, vol. 107, no. B11, Article ID 2300.

Bragina, L.G. and Bragin, N.Yu., Radiolaria from the upper Cretaceous (Turonian-Conician) deposits of the Bel'bek river basin (SW Crimea), in *Sb. nauchn. tr., Paleontologicheskie issledovaniya v Ukraine: istoriya, sovremennoe sostoyanie i perspektivy* (Collection of Papers, Paleontological studies in Ukraine: history, present-day, state and prospects), Gozhik, P.F., Ed., Kiev: Nora-print, 2007, pp. 187–191.

Chadima, M. and Hrouda, F., Remasoft 3.0—a user-friendly paleomagnetic data browser and analyzer, *Trav. Geophys.,* 2006, vol. XXVII, pp. 20–21.

Coccioni, R. and Premoli Silva, I., Revised Upper Albian – Maastrichtian plankonitc foraminiferal biostratigraphy and magnetostratigraphy of the classical Tethyan Gubbio section (Italy), *Newsl. Stratigr.*, 2015, vol. 48, no. 1, pp. 47–90.

Cox, A., Latitude dependence of the angular dispersion of the geomagnetic field, *Geophys. J. R. Astron. Soc.*, 1970, vol. 20, pp. 253–269.

Dunlop, D.J., Theory and application of the Day plot ($M_{rs}/M_s$ versus $H_{cr}/H_c$). 1. Theoretical curves and tests using titanomagnetite data, *J. Geophys. Res.: Solid Earth*, 2002, vol. 107, no. B3, Article ID 2056. https://doi.org/10.1029/2001JB000486

Eremin, V.N., Nazarov, Kh., Ramazanov, S.A., and Fomin, V.A., Magnetostratigraphy of the reference section of the Upper Cretaceous of the Western Kopetdag (Kanavchay), *Izv. Akad. Nauk Turkm.*, 1995, no. 4, pp. 163–169.

Fetisova, A.M., Golubev, V.K., Veselovsky, R.V., and Balabanov, Yu.P., Paleomagnetism and magnetostratigraphy of Permian-Triassic reference sections in the central Russian plate: Zhukov ravine, Slukino, and Okskiy siyezd, *Russ. Geol. Geophys.,* 2022, vol. 63, no. 10, pp. 1162–1176.

Fomin, V.A. and Eremin, V.N., Magnetostratigraphy of Upper Cretaceous deposits in the southern regions of the USSR, in *Voprosy stratigrafii paleozoya, mezozoya i kainozoya* (Questions of stratigraphy of the Paleozoic, Mesozoic and Cenozoic), Kuleva, G.V. and Ochev, V.G., Eds., Saratov: SGU, 1993, pp. 134–142.

Gale, A., Batenburg, S., Coccioni, R., Dubicka, Z., Erba, E., Falzoni, F., Haggart, J., Hasegawa, T., Ifrim, C., Jarvis, I., Jenkyns, H., Jurowska, A., Kennedy, J., Maron, M., Muttoni, G., et al., The global boundary stratotype section and point (GSSP) of the Campanian Stage at Bottaccione (Gubbio, Italy) and its auxiliary sections: Seaford Head (UK), Bocieniec (Poland), Postalm (Austria), Smoky Hill, Kansas (U.S.A), Tepayac (Mexico), *Episodes*, vol. 46, no. 3, pp. 451–490.

Gnibidenko, Z.N., Lebedeva, N.K., and Shurygin, B.N., A regional Upper Cretaceous magnetostratigraphic section of southern West Siberia (Omsk depression), *Dokl. Earth Sci.*, 2014, vol. 458, no. 1, pp. 1107–1111.

Gradstein, F.M., Ogg, J.G., Schmitz, M.B., and Ogg, G.M., *Geologic Time Scale 2020*, in 2 vols., Amsterdam: Elsevier, 2020.

Guzhikova, A.A., First magnetostratigraphic data on the Maastrichtian of Crimean Mountains (Bakhchisaray Region), *Izv. Saratov. Univ. Nov. Ser. Ser. Nauki Zemle*, 2019, vol. 18, no. 1, pp. 41–49.

Guzhikov, A.Yu. and Feduleev, D.V., Paleomagnetism of the Coniacian-Santonian deposits of the southwest Crimea, *Mater. XXV yubileinoi Vseross. shk.-semin. mezhdunar. uchastiem "Paleomagnetizm i magnetizm gornykh porod"* (Proc. XXV Jubilee All-Russ. Workshop Int. Participation "Paleomagnetism and Rocks Magnetism"), Moscow–Borok, 2019, Yaroslavl: Filigran', 2019, pp. 103–107.

Guzhikov, A.Yu., Molostovskii, E.A., Nazarov, Kh., Fomin, V.A., Baraboshkin, E.Yu., and Kopaevich, L.F., Magnetostratigraphic data on the Upper Cretaceous of Tuarkyr (Turkmenistan) and their implications for the general paleomagnetic time scale, *Izv., Phys. Solid Earth*, 2003, vol. 49, no. 9, pp. 728–740.

Guzhikov, A.Yu., Baraboshkin, E.Yu., and Fomin, V.A., Cretaceous polarity scale: modern status, problems of construction and outlook of development, in *Sb. nauchn. tr., Melovaya Sistema Rossii i blizhnego zarubezhya: problem stratigrafii i paleogeografii* (Collection of Papers, Cretaceous System of Russia and Neighboring Countries: Problems of Stratigraphy and Paleogeography), Pervushov, E.M., Ed., Saratov: Saratov. Univer., 2007, pp. 69–86.

Guzhikova, A.A., Guzhikov, A.Y., Pervushov, E.M., Ryabov, I.P., and Surinskiy, A.M., Existence of the reversal polarity zones in Turonian-Coniacian from the lower Volga (Russia): New data, Ch. 25 of *Recent Advances in Rock Magnetism, Environmental Magnetism and Paleomagnetism*, Nurgaliev, D., Shcherbakov, V., Kosterov, A., and Spassov, S., Eds., Springer Geophysics, Kazan: Springer, 2019, pp. 353–369.

Guzhikova, A.A., Pervushov, E. M., Ryabov, I.P., and Fomin, V.A., The reversal polarity zone in Turonian-Coniacian of the northern end of DonoMedvediza dislocations, *Izv. Sarat. Univ. Nov. Ser. Ser. Nauki Zemle,* 2020, vol. 20, iss. 4, pp. 262–277. https://doi.org/10.18500/1819-7663-2020-20-4-262-277

Guzhikova, A.A., Ryabov, I.P., and Kopaevich, L.F., New paleomagnetic and microfaunistic data on the Turonian-Santonian section "Aksu-Dere" (southwestern Crimea), *Mater. X Vseross. soveshch. "Melovaya sistema Rossii i blizhnego zarubezh'ya: problemy stratigrafii i paleogeografii"* (Proc. X All-Russ. Conf. "Cretaceous System of Russia and the Near Abroad: Problems of Stratigraphy and Paleogeography"), Baraboshkin, E.Yu. and Guzhikov, A.Yu., Eds., Magadan, 2020, Magadan: MAOBTI, 2020, pp. 81–84.

Guzhikov, A.Yu., Baraboshkin, E.Yu., Aleksandrova, G.N., Ryabov, I.P., Ustinova, M.A., Kopaevich, L.F., Mirantsev, G.V., Kuznetsov, A.B., Fokin, P.A., and Kosorukov, V.L., Bio-, chemo-, and magnetostratigraphy of the Santonian–Campanian boundary in the Kudrino and Aksu-Dere sections, (SW Crimea): Problems of global correlation and selection of the lower boundary stratotype of the Campanian. 1. Geological framework, sedimentology, biostratigraphy, *Stratigr. Geol. Correl.*, 2021a, vol. 29, no. 4, pp. 450–494.

Guzhikov, A.Yu., Baraboshkin, E.Yu., Aleksandrova, G.N., Ryabov, I.P., Ustinova, M.A., Kopaevich, L.F., Mirantsev, G.V., Kuznetsov, A.B., Fokin, P.A., and Kosorukov, V.L., Bio-, chemo-, and magnetostratigraphy of the Santonian–Campanian boundary in the Kudrino and Aksu-Dere sections (Southwestern Crimea): Problems of global correlation and selection of the lower boundary stratotype of the Campanian. 2. Magneto- and chemostratigraphy, discussion, *Stratigr. Geol. Correl.*, 2021b, vol. 29, no. 5, pp. 518–547.

Guzhikova, A.A., Grishchenko, V.A., Fomin, V.A., Baraboshkin, E.Yu., and Shelepov, D.A., Magnetostratigraphy of Turonian–Santonian strata on the Samara right bank, *Izv. Sarat. Univ. Nov. Ser. Ser. Nauki Zemle,* 2021, vol. 21, iss. 4, pp. 248–263. https://doi.org/10.18500/1819-7663-2021-21-4-248-263

Guzhikova, A.A., Guzhikov, A.Yu., and Ryabov, I.P., Paleomagnetic data on the Upper Cretaceous of the Crimean Mountains: arguments in favor of the existence of a long era of anomalous geomagnetic field regime in the Turonian-Santonian, in *Geologicheskie nauki—2021: Materialy Vse-*

*ross. nauchno-prakt. konf.* (Geological Sciences—2021: Proc. All-Russ. Research and Technical Conf.), Fomin, V.A. and Pimenov, M.V., Eds., Saratov, 2021, Saratov: Tekhno-Dekor, 2021, pp. 66–69.

Jacobs, J.A., Geomagnetic excursion, in *Encyclopedia of Geomagnetism and Paleomagnetism*, Dordrecht: Springer, 2007, pp. 311–312.

Khramov, A.N. and Shkatova, V.K., *Obshchaya magnitostratigraficheskaya shkala polyarnosti fanerozoya. Dopolneniya k stratigraficheskomu kodeksu Rossii* (General Magnetostratigraphic Polarity Scale of the Phanerozoic. Additions to the Russian Stratigraphic Code), St. Petersburg: VSEGEI, 2000, pp. 24–45.

Khramov, A.N., Goncharov, G.I., Komissarova, R.A., Pisarevskii, S.A., Pogarskaya, I.A., Rzhevskii, Yu.S., Rodionov, V.P., and Slautsitais, I.P., *Paleomagnitologiya (Paleomagnetology)*, Khramov, A.N., Ed., Leningrad: Nedra, 1982.

Klikushin, V.G., Turonian, Coniacian and Santonian deposits of the Belbek river valley in Crimea, *Byull. Mosk. O-va. Ispyt. Prir., Otd. Geol.*, 1985, vol. 60, iss. 2, pp. 69–81.

Kopaevich, L.F. and Valashchik, I., Subdivision of the Turonian-Coniacian deposits of the Aksudere section into inocerams and foraminifera, *Vestn. Mosk. Univ., Ser. 4: Geol.*, 1993, no. 5, pp. 70–82.

Kopaevich, L.F. and Walaszczyk, I.P., An integrated inoceramid/foraminiferal biostratigraphy of the Turonian and Coniacian strata in south-western Crimea, Soviet Union, *Acta Geol. Polon.*, 1990, vol. 40, nos. 1–2, pp. 83–96.

Kurazhkovskii, A.Yu., Kurazhkovskaya, N.A., and Klain, B.I., Spectrum of quasiperiodic variations in the paloemagnetic activity in the Phanerozoic, *Russ. Geol. Geophys.,* 2022, vol. 63, no. 11, pp. 1261–1269.

Lebedev, I.E., Bobrovnikova, E.M., Tikhomirov, P.L., Eid, B., Lhuillier, F., and Pavlov, V.E., Amplitude of secular geomagnetic variation in Late Cretaceous based on paleomagnetic studies of the Okhotsk–Chukotka volcanic belt from upper reaches of Malyi Anyui river, West Chukotka, *Izv., Phys. Solid Earth*, 2022, vol. 58, no. 2, pp. 185–202.

McElhinny, M.W. and McFadden, P.L., Palaeosecular variation over the past 5 Myr based on a new generalized database, *Geophys. J. Int.*, 1997, vol. 131, no. 2, pp. 240–252.

McFadden, P.L., A new fold test for palaeomagnetic studies, *Geophys. J. Int.*, 1990, vol. 103, no. 1, pp. 163–169.

Montgomery, P., Hailwood, E.A., Gale, A.S., and Burnett, J.A., The magnetostratigraphy of Coniacian–Late Campanian chalk sequences in southern England, *Earth Planet. Sci. Lett.,* 1998, vol. 156, nos. 3-4, pp. 209–224.

Pecherskii, D.M., *Paleomagnitologiya, petromagnitologiya i geologiya. Slovar'-spravochnik glya sosedei po spetsial'nosti* (Palaeomagnetology, Petromagnetology and Geology. Dictionary-Reference Book for Neighbors by Specialty), 2010. http://paleomag.ifz.ru/books/Pechersky.htm.

Pechersky, D.M. and Safonov, V.A., Palinspastic reconstruction of the Crimea Mountains position in the Middle Jurassic - Early Cretaceous obtained by paleomagnetic data, *Geotektonika,* 1993, no. 1, pp. 96–105.

Plotnikova, L.F., Bogaets, A.T., Bondarenko, V.G., and Korbut, E.B., Cretaceous system. Upper section, in *Geologiya shel'fa USSR. Stratigrafiya (shel'f i poberezh'ya Chernogo morya)* (Geology of the USSR Shelf. Stratigraphy (Shelf and Coasts of the Black Sea)), Teslenko, Yu.V., Ed., Kiev: Naukova Dumka, 1984, pp. 74–84.

Shcherbinina, E.A. and Gavrilov, Yu.O., Zonal division of Cenomanian–Santonian deposits of the Southwestern Crimea based on nannoplankton, in *Sb. nauchn. tr., Melovaya Sistema Rossii i blizhnego zarubezhya: problem stratigrafii i paleogeografii.* (Collection of Papers, Cretaceous System of Russia and cis Countries: Problems of Stratigraphy and Paleogeography), Baraboshkin, E.Yu., Ed., Simferopol: Chernomopress, 2016, pp. 292–294.

Shipunov, S.V., New fold test in paleomagnetism (rehabilitation of the mean test), *Izv., Phys. Solid Earth*, 1995, vol. 31, no. 4, pp. 342–348.

Solodovnikov, G.M., Determination of the geomagnetic field intensity in the Santonian-Coniacian (Upper Cretaceous) from an effusive section in Azerbaijan, *Izv., Phys. Solid Earth*, 2001, vol. 37, no. 7, pp. 600–605.

Valet, J.-P. and Herrero-Bervera, E., Geomagnetic reversals, archives, in *Encyclopedia of Geomagnetism and Paleomagnetism*, Dordrecht: Springer, 2007, pp. 339–344.

Van der Voo, R., *Paleomagnetism of the Atlantic, Tethys and Iapetus Oceans*, Cambridge: Cambridge Univ. press, 1993.

Yudin, V.V., Tectonics of the Belbek region in Crimea, *Uch. Zap. KFU im. V.I.Vernadskogo. Georg. Geol.*, 2020, vol. 6 (72), no. 2, pp. 338–360.

*Translated by M. Nazarenko*

**Publisher's Note.** Pleiades Publishing remains neutral with regard to jurisdictional claims in published maps and institutional affiliations.